Essentiality of c-di-AMP in *Bacillus subtilis*: Bypassing mutations converge in potassium and glutamate homeostasis

Larissa Krüger [a], Christina Herzberg [a], Hermann Rath [b], Tiago Pedreira [a], Anja Poehlein [c], Jan Gundlach [a], Rolf Daniel [c], Uwe Völker [b], Ulrike Mäder [b], and Jörg Stülke [a]*

[a] Department of General Microbiology, GZMB, Georg-August-University Göttingen, Germany

[b] Interfaculty Institute for Genetics and Functional Genomics, University Medicine Greifswald, Greifswald, Germany

[c] Department of Genomic and Applied Microbiology, GZMB, Georg-August-University Göttingen, Germany

Running head: Bypasses of cyclic di-AMP essentiality in *B. subtilis*

* Corresponding author:

Jörg Stülke, jstuelk@gwdg.de

ABSTRACT

In order to adjust to changing environmental conditions, bacteria use nucleotide second messengers to transduce external signals and translate them into a specific cellular response. Cyclic di-adenosine monophosphate (c-di-AMP) is the only known essential nucleotide second messenger. In addition to the well-established role of this second messenger in the control of potassium homeostasis, we observed that glutamate is as toxic as potassium for a c-di-AMP-free strain of the Gram-positive model bacterium *Bacillus subtilis*. In this work, we isolated suppressor mutants that allow growth of a c-di-AMP-free strain under these toxic conditions. Characterization of glutamate resistant suppressors revealed that they contain pairs of mutations, in most cases affecting glutamate and potassium homeostasis. Among these mutations, several independent mutations affected a novel glutamate transporter, AimA (Amino acid importer A, formerly YbeC). This protein is the major transporter for glutamate and serine in *B. subtilis*. Unexpectedly, some of the isolated suppressor mutants could suppress glutamate toxicity by a combination of mutations that affect phospholipid biosynthesis and a specific gain-of-function mutation of a mechanosensitive channel of small conductance (YfkC) suggesting the acquisition of a device for glutamate export. Cultivation of the c-di-AMP-free strain on complex medium was an even greater challenge because the amounts of potassium, glutamate, and other osmolytes are substantially higher than in minimal medium. Suppressor mutants viable on complex medium could only be isolated under anaerobic conditions if one of the two c-di-AMP receptor proteins, DarA or DarB, was absent. Also on complex medium, potassium and osmolyte toxicity are the major bottlenecks for the growth of *B. subtilis* in the absence of c-di-AMP. Our results indicate that the essentiality of c-di-AMP in *B. subtilis* is caused by the global impact of the second messenger nucleotide on different aspects of cellular physiology.

AUTHOR SUMMARY

Bacteria are exposed to constantly changing environmental conditions. In order to respond to these changes, they use nucleotide second messengers to transduce external signals and translate them into a specific cellular response. Among the repertoire of bacterial second messenger nucleotides, cyclic di-AMP (c-di-AMP) stands out as it is the only second messenger that is essential for the bacteria that produce it, including the Gram-positive model organism *Bacillus subtilis*. C-di-AMP plays a major role in the control of potassium homeostasis, and we found that glutamate is toxic to a *B. subtilis* strain lacking c-di-AMP to the same extent as potassium. These toxic conditions were the starting point for an extensive suppressor analysis, which led to the identification of a novel glutamate transporter (AimA). If the *B. subtilis* strain lacking c-di-AMP was cultivated on complex medium, the isolation of suppressor mutants was only possible under anaerobic conditions and if either of the two c-di-AMP-binding signal transduction proteins was absent. This suggests that these proteins are a major burden for the cell on complex medium in their c-di-AMP free state. Our result underline the complexity of c-di-AMP signaling and propose new directions for research.

KEYWORDS

Glutamate, potassium, *Bacillus subtilis*, cyclic di-AMP, ion homeostasis, osmoprotection, essential genes

65 **INTRODUCTION**

66

67 To achieve appropriate responses to changing environmental conditions, all organisms use second
68 messengers which are formed in response to an environmental cue. In bacteria, specific mono- and
69 dinucleotides play a particularly important role as second messengers [1]. The common nucleotide
70 second messengers cyclic AMP, cyclic di-GMP (c-di-GMP), and guanosine tetra/pentaphosphate
71 ((p)ppGpp) are used to prioritize the utilization of carbon sources and to regulate virulence, to control
72 the choice between sessile and motile lifestyles, and to downregulate essential cellular functions upon
73 amino acid starvation, respectively [2 - 7]. The more recently discovered second messenger cyclic di-
74 AMP is unique in several respects. First, this nucleotide is essential in many bacteria that produce it,
75 suggesting that this molecule plays a role in central cellular activities. Essentiality of c-di-AMP has been
76 observed in many Firmicutes, such as *Bacillus subtilis*, *Listeria monocytogenes*, *Streptococcus*
77 *agalactiae*, and *Staphylococcus aureus*, but also in the genome-reduced bacterium *Mycoplasma*
78 *pneumoniae* and in *Chlamydia trachomatis* [8 - 14]. Second, c-di-AMP is toxic if it accumulates in the
79 cells, and in many bacteria this accumulation results in strongly increased stress sensititvity [9, 15 –
80 19]. Third, c-di-AMP can bind to proteins and the mRNA molecules encoding them to control both the
81 expression and the activity of certain proteins, as in the case of the *B. subtilis* potassium transporters
82 KtrAB and KimA [20 - 23]. Last, but not least, c-di-AMP is not intrinsically present in eukaryotic
83 organisms, and the presence of the molecule is an indication for infection with pathogenic bacteria.
84 Indeed, c-di-AMP is recognized by the human immune system. It binds the STING protein thus resulting
85 the induction of an innate immune response [10].

86 The essentiality and toxicity of c-di-AMP for many bacteria have induced a great interest in
87 understanding the reasons behind it. Classically, genes were regarded to be essential if they were
88 absolutely needed for growth under optimal growth conditions, typically on complex medium at 37°C
89 [24 - 26]. However, many genes are not described as being essential because there may be paralogues
90 that encode very similar functions as has been described for the c-di-AMP producing diadenylate

91 cyclases in *B. subtilis* [8, 9]. In some cases, one essential function can be carried out by very different
92 proteins, and such genes are essential only under specific conditions, *i. e*. the absence of amino acids
93 from the medium makes the corresponding biosynthetic genes essential. These genes have been called
94 conditional essential genes. Finally, some genes may not be essential but their loss would cause a
95 substantial decrease of fitness for the cells, resulting either in the disappearance of such mutants or in
96 the acquisition of suppressor mutations. Such genes or proteins have been designated quasi-essential,
97 and the effect of their loss has been studied for the *B. subtilis* DNA topoisomerase TopA, the
98 endoribonuclease RNase Y, and the modulator of lipid biosynthesis, YqhY [27 - 29]. Very recently,
99 essential processes have been ranked on a global scale for the first time by the determination of the
100 speed of death of mutants [30].

101 Two lines of research have provided important insights into the reasons of c-di-AMP
102 essentiality. Studies to identify target molecules that interact with c-di-AMP demonstrated that many
103 proteins involved in potassium and osmolyte homeostasis – both transporters and their regulators –
104 are controlled by c-di-AMP to limit the intracellular concentrations of potassium and osmotically
105 compatible compounds to physiologically reasonable levels [11, 13, 23, 31 - 38]. In a complementary
106 approach, suppressor mutants of bacterial strains that either lack or accumulate c-di-AMP have been
107 studied. These analyses revealed that c-di-AMP is conditionally essential in *L. monocytogenes*, *S.*
108 *aureus* and *B. subtilis*. While the nucleotide is required for growth on complex media, it is dispensable
109 on minimal media [21, 39, 40]. For a *B. subtilis* mutant lacking c-di-AMP, growth was only possible on
110 minimal medium as long as the potassium concentration in the medium is low and glutamate is not
111 present [21, 41]. On complex medium, the lack of c-di-AMP leads to an accumulation of (p)ppGpp [39],
112 the second messenger that results in a global reprogramming of transcription, translation, and
113 metabolism upon amino acid starvation. Inactivation of the enzymes that produce (p)ppGpp restores
114 the viability of the strain lacking c-di-AMP on complex medium. The accumulation of (p)ppGpp leads
115 to the inability of the transcription factor CodY to bind to its targets and thus in deregulation of a large
116 regulon that includes many genes for osmolyte uptake and amino acid metabolism, and this

117 uncontrolled expression of the CodY regulon is responsible for the essentiality of c-di-AMP for *L.*
118 *monocytogenes* on complex media [39]. In *S. aureus*, c-di-AMP is dispensable for growth on complex
119 medium under anaerobic conditions or when the bacteria acquire suppressor mutations that affect
120 osmolyte or glutamate uptake [40, 42]. Both types of studies support the idea that the control of
121 potassium and osmolyte homeostasis is the central essential function of c-di-AMP in many bacteria
122 that produce it [43 - 45].

123 We are interested in c-di-AMP signaling in the model organism *B. subtilis*. In contrast to *S.*
124 *aureus* or *L. monocytogenes*, *B. subtilis* encodes three diadenylate cyclases that produce c-di-AMP, the
125 constitutively expressed enzymes CdaA and DisA, and the sporulation-specific enzyme CdaS [9, 46].
126 Mutants lacking both the *cdaA* and *disA* genes that encode the constitutive enzymes are not viable on
127 complex medium and tolerate only very low potassium concentrations and no glutamate in minimal
128 medium. In *B. subtilis*, c-di-AMP binds to two signal transduction proteins, DarA and DarB, to several
129 potassium, osmolyte and magnesium transporters, as well as to the riboswitch that controls the
130 expression of the high affinity potassium transporters KtrAB and KimA [20, 23, 47].

131 To get a better understanding of the global role of c-di-AMP for the physiology of *B. subtilis*,
132 we performed extensive suppressor analysis of strains lacking c-di-AMP that had adapted to tolerate
133 the presence of glutamate or that are viable on complex medium. These suppressor analyses were
134 complemented by a transcriptome analysis to understand the roles of glutamate and potassium as well
135 as of c-di-AMP for global gene expression in *B. subtilis*. Our results indicate that the adaptation to
136 either glutamate or complex medium usually requires the simultaneous presence of multiple
137 suppressor mutations that often affect potassium uptake, osmolyte uptake, or glutamate metabolism.
138 Moreover, a mechanosensitive channel and phospholipid biosynthesis play an important role in the
139 sensitivity of a strain lacking c-di-AMP to glutamate. Strikingly, this study identified the amino acid
140 transporter YbeC (renamed AimA, amino acid importer A) as the major glutamate transporter in *B.*
141 *subtilis*. On complex medium, the c-di-AMP-binding signal transduction proteins DarA and DarB seem
142 to be toxic in the absence of c-di-AMP, and only in their absence we could isolate suppressor mutants.

143 The obtained results shed light on the complexicity of c-di-AMP essentiality and open new directions
144 of research.
145
146 **RESULTS**
147
148 **Growth of a strain lacking c-di-AMP in the presence of glutamate requires distinct combinations of**
149 **suppressor mutations**
150
151 A *B. subtilis* strain lacking all three diadenylate cyclases is unable to grow at potassium concentrations
152 of 5 mM or higher or in the presence of glutamate (even at low potassium concentrations) [21, 41]. In
153 order to get more comprehensive insights into the toxicity of glutamate for the c-di-AMP-free strain
154 GP2222 (designated Δ*dac* from here on), we decided to isolate and study a larger set of suppressor
155 mutants that tolerate the presence of glutamate. For this purpose, we plated the Δ*dac* strain [21] on
156 MSSM medium containing glutamate (1% w/v) and a low concentration of potassium (0.1 mM KCl).
157 While suppressor mutants appear readily after overnight cultivation when potassium toxicity was the
158 growth-limiting problem [21], the toxicity of glutamate could only be overcome after several days.
159 Moreover, the number of suppressor mutants was strongly reduced as compared to selection in the
160 presence of potassium and ammonium as the nitrogen source. After four days at 37°C, 14 colonies
161 could be isolated (see Fig. 1, Δ*dac*). These strains were subjected to whole genome sequencing to
162 identify the responsible mutations (Table 1). The long time for suppressor mutations to appear can be
163 explained by each mutant harboring multiple mutations. In addition, this explains why the overall
164 number of suppressors was rather low.
165
166
167

168 **Table 1. Characterization of suppressor mutants derived from the Δ*dac* strain GP2222 in MSSM**

169 **minimal medium with glutamate and 0.1 mM KCl.** [1]

170

Strain	Genotype	Ammonium, 0.1 mM KCl	Ammonium, 5 mM KCl	Glutamate, 0.1 mM KCl	Glutamate, 5 mM KCl	LB
GP2840[2]	*ktrC* (fs) *plsC*-A61V *ndhF* (fs) *sigD*-G88D	+++	+++	+++	+++	-
GP3079	Δ(*abh-kinC-ykqA-ktrC*) *plsC*-L48P *yfkC*-R42W *fliP* (fs) *hbs*-I32T *ndoA*-G6S	++	+++	+++	+++	+++
GP3077	*ktrC* (fs) *aimA/glpQ* (trunc) *ybcC* (fs)	+++	+++	+++	+++	-
GP2841	*gudB*$^+$ *accC*-H298Y *fliG* (fs)	+	+	++	+	-
GP2842	*nhaK*-S187F *aimA* (fs)	+++	+++	++	+	-
GP3078	*plsC*-A61V *aimA*-T374M *ktrB*-G313D *sigD*-G88D	+++	+	+++	-	-
GP2849	*ybcC*-K722L, I724F *aimA* (fs)	+++	+++	+++	+++	-
GP2837	*plsC*-L48P *yfkC*-R42W *fliP* (fs)	+++	+++	+++	+++	+++
GP3099	*plsC*-L48P *yfkC*-R42W *fliP* (fs) *cotO*-I34F	+++	+	+++	-	-
GP3464	*plsC*-P110S *flhA* (fs)	++	++	++	-	++
GP2224	*yqeG* (fs) *aimA* (fs) *yqeV* (fs)	+++	+++	+++	+++	-
GP2838	*ndhF*-V237E, M241L, H242L, A243D, G244C, L245F ΔICEBs1 (*int-yddM*) *yoaI* (fs)	+++	++	++	++	++
GP3473	*ndhF* (fs) *aimA* (fs) *gudB*$^+$ *fliH* (fs) *yuiE*-G37V	++	++	++	-	-
GP3474	*ndhF* (fs) *aimA* (fs) *ykpA* (fs) *ktrC* (fs) *fliK* (fs)	++	+++	+++	+++	-

GP2839	*fliK* (fs) *rpoB*-Q109P *rbsB*-R175L	++	++	++	-	-

171

172 [1] Growth on different media was judged after plating on corresponding agar plates.

173 [2] This strain was isolated in a previous study [41].

174

175 As observed previously [41], three strains were affected in *ktrC*. In one of these strains
176 (GP3079), the genomic region from *abh* to *ktrC* was deleted resulting in reduced uptake of potassium
177 via KtrCD. Similarly, strain GP3078 has a mutation affecting the high-affinity potassium transporter
178 KtrB, and GP2842 also carries a mutation (*nhaK*) that affects potassium homeostasis. Interestingly, the
179 same mutation (NhaK-S187F) had been isolated in a suppressor screen of the Δ*dac* strain in the
180 presence of 5 mM potassium [21] indicating that the mutant protein has an increased activity in
181 potassium export.

182 As mentioned above, the suppressor strains usually had multiple mutations. Since we never
183 experienced the systematic acquisition of multiple mutations in prior suppressor screens [15, 27, 48 -
184 50], it seems likely that more than one mutation is required to achieve the suppression. Since the
185 selective pressure in our experiment was directed towards tolerating otherwise toxic glutamate, we
186 expected that the suppressor mutants would contain mutations affecting glutamate metabolism.
187 Indeed, the á priori cryptic glutamate dehydrogenase was decryptified by the deletion of nine base
188 pairs in two mutants (GP2841 and GP3473), thus allowing glutamate degradation [51, 52]. Moreover,
189 seven independently isolated mutants carried mutations affecting an amino acid transporter, YbeC.
190 This protein has recently been identified as the major serine transporter of *B. subtilis* [53], and it is
191 tempting to speculate that YbeC is the major glutamate transporter as well (see below). However,
192 seven of the isolated mutants did not carry any mutation that is easily linked to glutamate homeostasis.
193 The previously reported suppressor mutant GP2840 had mutations affecting PlsC, NdhF, and SigD (acyl-
194 ACP:1-acylglycerolphosphate acyltransferase, NADH dehydrogenase, Sigma factor σ^D, respectively) in

195 addition to the *ktrC* mutation [41]. Strikingly, *plsC* and *ndhF* are affected in six and four different
196 suppressor mutants respectively. Several mutants carried mutations affecting motility: In addition to
197 two *sigD* mutants, seven additional mutants carried mutations in flagellar genes that on one hand
198 depend on a functional SigD for their expression, and on the other hand are required for SigD activity
199 [54]. In addition, three of the 14 different independent suppressor mutants carry the same point
200 mutation in the *yfkC* gene, encoding a mechanosensitive channel that releases ions from the cell [55,
201 56]. This mutation results in a substitution of Arg-42 by a Trp residue.

202 We then tested the ability of the suppressor mutants to grow on minimal medium at low and
203 high potassium concentrations with ammonium or glutamate as the nitrogen source. Moreover, the
204 ability to grow on a complex medium was tested (see Table 1, S1 Fig.). Since the mutants were isolated
205 in the presence of glutamate and 0.1 mM potassium, it is not surprising that all strains grew on the
206 corresponding medium. Moreover, most of the strains were viable with ammonium as the single
207 nitrogen source irrespective of the potassium concentration. Most of the mutants were also capable
208 of growing at the elevated potassium concentration in the presence of glutamate. However, only four
209 of the 15 tested strains were viable on complex medium. Two of them grew well on LB and these
210 strains had the identical combination of mutations in *yfkC* and *plsC* (see Table 1, see below). This
211 suggests that the adaptation to complex medium requires more than resistance to potassium and
212 glutamate.

213

214 **Stepwise adaptation of a strain lacking c-di-AMP to growth on complex medium**

215

216 Most of the suppressor mutants that tolerate the presence of glutamate and potassium were unable
217 to grow on complex medium under standard laboratory conditions. The standard definition of
218 essentiality refers to optimal growth conditions, *i. e*. to a complex medium and growth at 37°C in the
219 presence of oxygen for *B. subtilis* [25, 26]. This prompted us to investigate the growth requirements of
220 the Δ*dac* mutant GP2222 more rigorously. First, we attempted to isolate suppressor mutants derived

221 from GP2222 under standard conditions as defined above. However, we never succeeded in isolating
222 a single suppressor mutant. A recent study on c-di-AMP essentiality in *S. aureus* revealed that the
223 nucleotide is dispensable under anaerobic conditions [40]. Therefore, we tried to isolate suppressor
224 mutants of GP2222 in the absence of oxygen. While the wild type strain *B. subtilis* 168 grew under
225 these conditions, again no suppressor mutants of the Δ*dac* strain could be isolated (see Fig. 2).

226 In *B. subtilis*, c-di-AMP binds two signal transduction proteins, DarA and DarB [23, 47]. In a
227 suppressor screen using a *L. monocytogenes* strain lacking c-di-AMP, several mutations in the
228 corresponding genes were observed [39]. We therefore constructed strains that lack both c-di-AMP
229 and either the *darA* or the *darB* gene, and used these strains to isolate suppressors on complex
230 medium under aerobic and anaerobic conditions. Again, no suppressors could be obtained under
231 aerobic conditions; however, we detected one and two suppressors for the Δ*dac* Δ*darA* and Δ*dac*
232 Δ*darB* mutants, respectively, under anaerobic conditions (see Fig. 2). Whole genome sequencing
233 revealed that the mutation present in the Δ*dac* Δ*darA* mutant changed Gly-11 of KtrC to a cysteine
234 residue. The suppressor mutants derived from the Δ*dac* Δ*darB* mutant had a frameshift in *ktrC*
235 resulting in the expression of a truncated KtrC protein or a mutation affecting the permease domain
236 OpuAB of the OpuA glycine betaine transporter [57], respectively (Fig. 2). These results strongly
237 support the idea that the accumulation of potassium or of osmoprotective compatible solutes is the
238 reason for the essentiality of c-di-AMP [39, 40, 43].

239 An initial characterization of these suppressor mutants revealed that they were viable under
240 anaerobic conditions, but not in the presence of oxygen. Therefore, we used the three strains for a
241 further round of suppressor isolation. Indeed, we were able to obtain suppressors that tolerate the
242 presence of oxygen for all three mutants (Fig. 2, S3 Fig.). Whole-genome sequencing revealed that the
243 initial suppressors with defective KtrC proteins had all acquired very specific mutations in the *kimA*
244 gene, encoding the major high-affinity potassium transporter KimA. In the mutant isolated from the
245 *darA ktrC* mutant, the absolutely conserved glycine in transmembrane helix 3 of KimA was deleted.
246 Helix 3 is essential for potassium binding of KimA [58]. All four independent suppressors isolated from

247 the Δ*dac* Δ*darB ktrC* mutant had a deletion of 11 amino acids in the transmembrane helix 9. Based on
248 the high conservation of the deleted residues, we conclude that the mutant KimA proteins were
249 inactive or less active than the wild type protein. Again, the *kimA* suppressor mutations were
250 accompanied by other mutations (see Fig. 2). In the suppressor mutant GP3010 derived from the Δ*dac*
251 Δ*darA ktrC* mutant, we found a 155 bp deletion that results in the truncation the global transcription
252 regulator for catabolic genes and operons, CcpA, and in the conversion of the start codon of *motP*,
253 encoding the Na^+-coupled MotP flagellar stator protein to a stop codon. For the Δ*dac* Δ*darB ktrC*
254 suppressor mutant, two aerobic suppressors were subjected to whole genome sequencing. In one
255 strain (GP2845), we found a point mutation in the *darA* gene that results in a substitution of the
256 conserved Val-100 residue by an alanine in the DarA protein. The second suppressor (GP3094) carried
257 mutations affecting the CodY transcription factor (G146V substitution) and the unknown SPβ phage
258 protein YonD (D255H). In two additional suppressor mutants, we found identical frameshift mutations
259 in *darA* that result in a truncation of the DarA protein after amino acid 64. Finally, we also characterized
260 an aerobic suppressor (GP2847) derived from the anaerobic Δ*dac* Δ*darB opuAB* suppressor mutant. In
261 this case, again a potassium channel subunit (KtrB) was inactivated as the result of a frameshift
262 mutation. Moreover, this strain carried a frameshift mutation in the essential *accA* gene encoding a
263 subunit of acetyl-CoA carboxylase that resulted in the formation of a truncation after amino acid 108
264 and mutations in the genes encoding the putative methylenomycin A exporter Mmr and the tRNA
265 methylthiotransferase YmcB. These results again highlight the importance of potassium homeostasis
266 for the adaptation of strains lacking c-di-AMP.

267 Taken together, a *B. subtilis* strain lacking c-di-AMP is only able to grow under standard
268 laboratory conditions if it acquires several suppressing mutations. The results of the two suppressor
269 screens in the presence of glutamate and directly on complex medium demonstrate a distinct selective
270 pressure under both conditions resulting in different sets of mutations that allow aerobic growth on
271 complex medium. The importance of the initial loss of the c-di-AMP receptor proteins DarA and DarB
272 for the direct adaptation to complex medium demonstrates that these proteins interfere with the

273 growth of *B. subtilis* if they are present in the ligand-free apo-state. Indeed, apo-DarB was recently
274 shown to trigger growth-inhibitory (p)ppGpp synthesis by the Rel protein [59, 60]. For DarA, this is the
275 first time that a phenotype for the corresponding mutant is reported. The repeated isolation of
276 mutations affecting potassium uptake even in iterative cycles of suppressor screens highlights the
277 severe toxicity of potassium for *B. subtilis* in the absence of c-di-AMP.
278
279 **A global transcription study of the regulatory effects of potassium, glutamate, and c-di-AMP**
280
281 In order to obtain deeper insights into the physiological role of c-di-AMP, we decided to study the
282 impact of a lack of this second messenger on global gene expression by a transcriptome analysis as a
283 complementary approach to the suppressor analysis. Since c-di-AMP has been implicated in the
284 interplay of potassium and glutamate homeostasis, we analysed the global gene expression for the
285 wild type strain *B. subtilis* 168 at low (0.1 mM) and high (5 mM) potassium concentrations and in the
286 presence of ammonium and glutamate as the nitrogen source (S1 Supporting Information). Moreover,
287 we used the c-di-AMP free strain (Δ*dac*) GP2222 as well as the isogenic suppressor mutant GP2223
288 that is able to grow at 5 mM potassium (see Fig. 3 for the regulatory network and S1 Table). Strikingly,
289 expression of several genes involved in fermentation and respiration was strongly reduced in the
290 absence of c-di-AMP. The *ldh-lctP* and *cydABCD* operons encoding lactate dehydrogenase and the
291 lactate exporter as well as the terminal quinole oxidase, are repressed by the NADH-responsive
292 transcription factor Rex [61, 62]. The about 100-fold repression of these genes in the absence of c-di-
293 AMP suggests that the NADH levels are reduced in the mutant. This conclusion is also supported by
294 the increased expression (seven-fold) of the *ndhF-ybcC* operon (see S1 Table) which codes for a NADH
295 dehydrogenase and thus also contributes to the oxidation of $NADH_2$ to NAD [63]. Importantly, the *ndhF*
296 gene and its downstream gene *ybcC* were affected in several of the suppressor mutants suggesting
297 that these mutations counteract the increased expression of the conserved *ndhF-ybcC* operon. In
298 addition to genes of the Rex regulon, genes of the SigO regulon that are involved in the response to

299 acid stress [64] and several competence genes were severely reduced in the Δ*dac* mutant GP2222. The
300 strong reduction of competence gene expression in response to the absence of c-di-AMP suggests that
301 this second messenger might be required for genetic competence and transformation in *B. subtilis*. To
302 test this hypothesis, we attempted transformation of strain GP2222 using chromosomal DNA. No
303 transformants were obtained, whereas the control strain 168 was efficiently transformable. Thus, the
304 lack of c-di-AMP results in a loss of genetic competence as a result of reduced competence gene
305 expression.

306 It has been shown before that the expression of the high affinity potassium uptake systems
307 KtrAB and KimA is repressed in the presence of potassium via a c-di-AMP sensitive riboswitch [20 - 22].
308 In agreement with those results, these genes were most strongly repressed by potassium in our
309 analysis in the wild type strain 168. The expression of the *kimA* transporter gene was 112- and 17-fold
310 repressed at 5 mM potassium in the presence of glutamate or ammonium, respectively; whereas the
311 expression of the *ktrAB* channel operon was reduced 29- and 4-fold, respectively (see S2 Table). As
312 expected, the expression of both *kimA* and *ktrAB* is increased in the absence of c-di-AMP; however,
313 both genes are still repressed by potassium (eight- and five-fold, respectively), indicating a second, c-
314 di-AMP independent mechanism of transcriptional regulation of these potassium transport systems.
315 The particular importance of potassium for the cell and for KimA as a major high-affinity transporter is
316 highlighted by the fact that the *kimA* gene belongs to the most strongly expressed genes at 0.1 mM
317 potassium (position #50 in the presence of glutamate), and that it is even the most strongly expressed
318 transporter in *B. subtilis* under these conditions (see
319 https://www.ncbi.nlm.nih.gov/geo/query/acc.cgi?acc=GSE156738 for the full data set).

320 Taken together, the global transcription analysis supported the idea that c-di-AMP is involved
321 in multiple cellular functions. Moreover, the analysis confirmed a particular role of genes involved in
322 controlling NADH homeostasis, as already suggested by the suppressor analysis and by the differential
323 effects of aerobic and anaerobic conditions to allow suppressor formation of the strains lacking c-di-
324 AMP.

325

326 **The mechanosensitive channel YfkC contributes to the glutamate sensitivity of a c-di-AMP free strain**

327

328 Three of the suppressor mutants isolated in the presence of glutamate carry mutations affecting the
329 mechanosensitive channel of small conductance, YfkC (see Table 1). Strikingly, all three independently
330 isolated mutants carry precisely the same mutation that results in a R42W substitution in the protein
331 (see S4 Fig.). This residue is located at the end of the first trans-membrane helix [65] and the mutation
332 may affect the relative positioning of the trans-membrane helices 1 and 2. Another striking feature is
333 that this mutation is in all three cases accompanied by point mutations in the *plsC* gene (see below).
334 The presence of the same amino acid substitution in YfkC in all three strains suggested that this
335 mutation resulted in a gain of function rather than in a loss of YfkC activity (from here on, we designate
336 the mutant allele *yfkC**, the protein YfkC*). To address this question, we constructed Δ*dac* Δ*yfkC* and
337 Δ*dac yfkC** strains lacking all diadenylate cyclases and assayed the growth of these strains on minimal
338 medium containing glutamate or ammonium as the nitrogen source at high and low potassium
339 concentrations (see Fig. 4). Both strains were viable when cultivated on plates containing ammonium
340 and 0.1 mM potassium whereas they were unable to grow in the presence of glutamate or at the high
341 potassium concentration. These observations indicate that neither the deletion of the *yfkC* gene nor
342 *yfkC** mutation alone were sufficient to allow suppression of the glutamate and potassium toxicity of
343 the Δ*dac* mutant. To address this issue further, we attempted the isolation of suppressor mutants from
344 the Δ*dac* strain either lacking *yfkC* or carrying the *yfkC** allele in the presence of glutamate. No
345 suppressor mutants could be isolated from the Δ*dac* Δ*yfkC* mutant, whereas two suppressor mutants
346 were obtained from the Δ*dac yfkC** mutant (see Fig. 1). This observation supports the idea that the
347 specific R42W substitution of YfkC* is a prerequisite for the adaptation of the c-di-AMP-free strain to
348 growth in the presence of glutamate. Whole genome sequencing of the two glutamate-resistant
349 suppressor mutants identified a mutation in *accA* in strain GP2850 (see below). This mutation supports
350 the requirement of paired mutations affecting *yfkC* and lipid biosynthesis. The second suppressor

351 strain, GP3105, carries mutations affecting the amino acid transporter YbeC, the CarB subunit of the
352 carbamoyl-phosphate synthetase, the endonuclease MutL and the polyketide synthase PksJ. Among
353 these mutations, the frameshift in the *ybeC* gene is likely the most relevant (see below). These
354 suppressor mutants were also tested for their growth in the presence of glutamate or increased
355 potassium concentrations (see Fig. 4). Both were viable in the presence of glutamate irrespective of
356 the potassium concentration. However, the growth in the presence of glutamate was much better in
357 the case of the *yfkC** *plsC* (L48P) mutant GP2837 (Fig. 4). Taken together, these results suggest that
358 the *yfkC** mutation in combination with the lipid biosynthetic or *ybeC* mutations is rather specific for
359 the protection of the Δ*dac* mutant from glutamate toxicity. In the growth assay, we also included the
360 Δ*dac nhaK* (S187F) mutant that has been isolated for resistance to potassium [21]. As expected, this
361 strain grew at 5 mM potassium but was as sensitive to glutamate as the original Δ*dac* mutant, however
362 we observed the rapid formation of suppressor mutants in the presence of glutamate (see Fig. 4, see
363 below). As the NhaK allele used in this experiment is thought to exhibit increased potassium export
364 activity [21], it is tempting to speculate the mutant mechanosensitive channel YfkC* is able to export
365 glutamate to overcome the toxicity of this amino acid.
366
367 **A reduction of phospholipid biosynthesis helps to overcome the lack of c-di-AMP**
368
369 The analysis of suppressor mutants that were viable in the presence of glutamate or on complex
370 medium identified several mutations that affect proteins involved in phospholipid biosynthesis, *i. e*.
371 AccA, AccC, and PlsC (see Fig. 1, Fig. 2, Table 1). The *accA* and *accC* genes encode subunits of the
372 essential acetyl-CoA carboxylase. Unexpectedly, a frameshift had occurred in the *accA* gene of strain
373 GP2847. Since malonyl-CoA synthesis is the essential first step in fatty acid and phospholipid
374 biosynthesis, it is likely that this mutation can be intrinsically suppressed and thus does not result in a
375 complete loss of AccA synthesis. The *accA* mutation isolated in the Δ*dac yfkC** mutant results in an
376 A229V substitution in the active site of the enzyme [66, 67] (see S5 Fig.). For AccC, the mutation

377 (H298Y) is located in the highly conserved active site motif of the enzyme (S5 Fig). The localization of
378 these mutations strongly suggests that the initial step of lipid biosynthesis, the formation of malonyl-
379 CoA, is severely impaired in the suppressor mutants.

380 PlsC is the acyl-ACP:1-acylglycerolphosphate acyltransferase that catalyzes the formation of
381 phosphatidic acid in the synthesis of phospholipids. Interestingly, the *plsC* gene is essential for the
382 growth of *B. subtilis*. In agreement with this essentiality, none of the three different mutations in the
383 six independent mutants results in a frame shift or a deletion. Instead, residue L48 is replaced by a
384 proline in three independently isolated mutants, A61 by a valine in two mutants, and P110 by serine
385 in one mutant. All three residues are located in functionally important regions of the protein. L48 is
386 close to the HXXXXD motif, which is part the active site of the enzyme. Similarly, A61 and P110 are in
387 very close proximity to the active center of the enzyme [68] (S6 Fig). The location of all three mutations
388 in the immediate vicinity of the active center as well as the fact that the mutations affect conserved
389 residues suggest that they result in a reduced PlsC activity, and thus in reduced phospholipid
390 biosynthesis.

391 The requirement of the Δ*dac yfkC** mutant for an additional mutation reducing lipid
392 biosynthesis to allow growth in the presence of glutamate suggests that the membrane properties are
393 important for controlling cellular glutamate homeostasis. This conclusion is supported by the well-
394 established functional interaction between mechanosensitive channels and lipid molecules [69, 70]. It
395 is tempting to speculate that the combination of altered lipid composition and the mutation in the
396 trans-membrane helix of YfkC results in a change of channel properties that facilitates the export of
397 glutamate by YfkC.

398

399 **AimA (YbeC) is a novel major glutamate transporter**

400

401 The acquisition of suppressor mutations that provide resistance to glutamate to the Δ*dac* mutant was
402 a rare event that took several days to occur (see above). However, we observed the rapid appearance

403 of glutamate-resistant suppressor mutants if the strain already carried a *nhaK* mutation that facilitates
404 potassium export (see Fig. 4). To determine the requirements for glutamate resistance in more detail,
405 we isolated a set of 16 new suppressor mutants (see Fig. 1). Since the originally isolated suppressor
406 mutant GP2842 carried a combination of mutations in *nhaK* and the *ybeC* gene encoding an amino acid
407 transporter, we sequenced the *ybeC* allele in all glutamate-resistant suppressor mutants isolated from
408 the Δ*dac nhaK*(S187F) (from now on referred to as *nhaK** and NhaK* for the gene and protein,
409 respectively). Strikingly, all 16 strains carried mutations in *ybeC*. Among these mutations are
410 frameshifts in ten strains, an insertion of 2 amino acids after residue 226 in one strain, and amino acid
411 substitutions in the remaining five strains (for details, see Table 2). The high number of mutants with
412 inactivated *ybeC* genes strongly suggests that the combination of NhaK* and loss of YbeC allows
413 growth of the Δ*dac* mutant in the presence of glutamate. To test this hypothesis, we deleted the *ybeC*
414 gene in the Δ*dac* mutant. The resulting strain, GP3054, was unable to grow in the presence of
415 glutamate, indicating that only the combination of the *nhaK** and the *ybeC* mutations conferred
416 resistance to glutamate to the Δ*dac* mutant.

417 Three lines of evidence suggest that YbeC is the major glutamate transporter of *B. subtilis*: (i)
418 We isolated seven independent mutants affected in *ybeC* in the initial screen for mutations conferring
419 glutamate resistance to the Δ*dac* strain, (ii) we reproducibly isolated a large number of *ybeC* mutants
420 based on the Δ*dac nhaK** mutant, and (iii) YbeC is an amino acid transporter of the amino acid-
421 polyamine-organocation (APC) superfamily. We have recently demonstrated that YbeC is the major
422 serine transporter of *B. subtilis* [53]. It is well established that many amino acid transporters can take
423 up multiple different amino acids. To test the possible role of YbeC in glutamate uptake, we first
424 attempted functional complementation in *E. coli* that is unable to grow with glutamate as the single
425 source of carbon and nitrogen due to the low activity of intrinsic glutamate transporters [71]. For this
426 purpose, we transformed *E. coli* JM109 with plasmid pGP2987 that carries the *ybeC* gene or with the
427 empty vector pWH844 [72]. The resulting transformants were tested for growth on minimal medium
428 with glucose and ammonium or with glutamate as the only source of carbon and nitrogen (see Fig. 5A).

429 Whereas both strains grew well with glucose and ammonium, the strain carrying the empty vector was
430 unable to utilize glutamate. In contrast, the expression of the *ybeC* gene allowed *E. coli* to use
431 glutamate as source of carbon and energy. These findings confirm that YbeC indeed is a glutamate
432 transporter. The protein and the gene were therefore renamed AimA and *aimA*, respectively (amino
433 acid importer A).

434 It is very striking that our suppressor screens for glutamate-resistant mutants often identified
435 AimA but never GltT or GltP, the two described glutamate transporters of *B. subtilis*. Therefore, we
436 analyzed the contributions of these proteins to glutamate uptake by comparing the growth of strains
437 expressing only one of the three proteins and a strain lacking all of them (see Fig. 5B). All tested strains
438 grew well in the presence of ammonium as the nitrogen source, reflecting their ability to synthesize
439 glutamate. The strain GP3071 lacking all three presumptive glutamate transporters was only viable at
440 high glutamate concentrations but not at 1 mM or 5 mM. This demonstrates that the bacteria need to
441 transport glutamate if no ammonium is available for its synthesis. Moreover, it demonstrates that
442 efficient glutamate transport is not possible in the absence of the three proteins. GP2818 expressing
443 GltT grew at the three tested glutamate concentrations confirming its role as glutamate transporter.
444 The strain GP2825 that expressed AimA as the only glutamate transporter did not grow at the lowest
445 tested glutamate concentration (1 mM), but this strain was able to grow at 5 mM and 20 mM
446 glutamate suggesting that AimA might be a low-affinity glutamate transporter. In contrast, the strain
447 expressing GltP was only viable at highest glutamate concentration as observed for strain GP3071
448 lacking all three proteins. This suggests that GltP plays only a very minor, if any role, in glutamate
449 uptake, and that yet another protein can transport glutamate at high concentrations.

450 To study the activities of AimA and GltT in glutamate transport in more detail, we assayed the
451 growth of strains expressing only one of these transporters at different glutamate concentrations (see
452 Fig. 5C, 5D). Moreover, we performed this experiment in the presence of 0.1 mM and 5 mM KCl in the
453 medium to see whether potassium has an effect on glutamate uptake as it has been observed with an
454 activating effect of glutamate on potassium uptake by KtrCD [41]. As control, we used strain GP3071

455 that lacks AimA, GltT, and GltP. The results were used to calculate apparent K_S values that reflect the
456 affinities of the transporters for glutamate. For GltT, we observed K_S values of 0.3 mM and 0.06 mM in
457 the presence of 0.1 and 5 mM potassium, respectively. These results are in good agreement with the
458 description of GltT as a high-affinity glutamate transporter [73]. Moreover, they show that the affinity
459 of GltT for glutamate is five-fold increased in the presence of high potassium concentrations. For AimA,
460 we determined apparent K_S values of 3.2 and 2.3 mM in the presence of 0.1 and 5 mM potassium,
461 respectively. In good agreement with the drop dilution assay, this suggests that AimA is a low-affinity
462 glutamate transporter, and that the affinity of AimA is not affected by the external potassium
463 concentration. The strain GP3071 lacking all known and suspected glutamate transporters grew only
464 at high glutamate concentrations. This suggests the presence of an additional transporter with very
465 low affinity for glutamate (apparent K_S values of 12.3 and 13.8 mM in the presence of 0.1 and 5 mM
466 potassium, respectively). Thus, AimA is the major glutamate transporter under standard growth
467 conditions when glutamate is not limiting in the medium.

468 The role of AimA as the major glutamate transporter is in excellent agreement with the
469 common isolation of glutamate-resistant Δ*dac aimA* mutants whereas no *gltT* mutants could be
470 isolated. Indeed, the Δ*dac* Δ*gltT* mutant was unable to grow in the presence of glutamate, but again a
471 suppressor mutant, GP3093, could be isolated (see Fig. 1). Not surprisingly, this strain carries a
472 mutation in *aimA* (Leu-419 Pro). Moreover, this strain carries frame-shift mutations in *ndhF* and *fliK*.
473 The paired occurrence of *aimA* and *ndhF* suppressor mutations has been observed several times
474 independently (see Table 1).

475 To get further insights into *gltP*, *gltT* and *aimA*, we determined the expression of these genes
476 based on the transcriptome analysis under the relevant conditions (see Fig. 5E). The expression of *gltP*
477 was very low under all tested conditions, which is in agreement with the observation that GltP does
478 not play a significant role in glutamate uptake. The expression of both GltT and AimA was significant.
479 In the presence of glutamate in the medium, the expression was reduced five- and two-fold for AimA
480 and GltT, respectively, at the high potassium concentration (5 mM). In the absence of glutamate, *aimA*

481 expression did not respond to the supply of potassium whereas the expression of *gltT* was about two-
482 fold increased at the increased potassium concentration. Thus, if glutamate is limiting, both the
483 expression of *gltT* and the affinity of the GltT protein for glutamate are increased by potassium.
484
485 **Adaptation of a Δ*dac* Δ*aimA* mutant to growth in the presence of glutamate**
486
487 To make the picture of the requirements for a Δ*dac* mutant to tolerate glutamate complete, we also
488 adapted a Δ*dac* Δ*aimA* mutant to the presence of glutamate. As described above, this mutant was not
489 viable in the presence of glutamate; however, we could isolate three glutamate-resistant suppressor
490 mutants (see Fig. 1). The mutations in these strains were identified by whole genome sequencing.
491 Interestingly, all three suppressor mutants had mutations affecting the essential translation elongation
492 factor G, in two strains (GP3101 and GP3103) the highly conserved Ala-579 was replaced by a Val (see
493 S7 Fig.). Ala-579 is located in immediate vicinity of a loop (Loop II) that is required for tRNA
494 translocation in the ribosome [74, 75], suggesting that the mutation interferes with translation. In the
495 third strain (GP3102) we found an A21T substitution. This residue is the immediate neighbour of Asp-
496 20, which binds the Mg^{2+} ion in the active site of the protein [76]. The presence of substitutions in
497 highly conserved and functionally important regions of FusA in all three suppressors suggests that
498 reduced translation efficiency helps the Δ*dac* Δ*aimA* mutant to adapt to the presence of glutamate. In
499 addition to the mutations in *fusA* each strain had a distinct additional mutation. Strain GP3101 had a
500 frameshift mutation in the *yqeG* gene encoding a putative HAD superfamily phosphatase [77], whereas
501 the two other strains carried point mutations affecting potassium homeostasis (*nhaK* and *ktrC* for
502 GP3102 and GP3103, respectively) again highlighting the toxicity of potassium in the presence of
503 glutamate. Moreover, GP3102 carried amino acid substitutions affecting SigA, the housekeeping sigma
504 factor (F281V) and MrpA (P397L), a subunit of the sodium exporter of *B. subtilis*, and GP3103 had a
505 point mutation affecting the quasi-essential DNA topoisomerase 1 TopA (K13N). The analysis of these
506 strains for growth in the presence of glutamate with 0.1 or 5 mM potassium revealed that all

507 suppressors were viable at both potassium concentrations, however, the suppression was most
508 efficient if the *yqeG* or *ktrC* genes were affected in addition to *aimA* (see S8 Fig.).
509
510 **DISCUSSION**
511
512 Cyclic di-AMP is essential f or many bacteria that produce this second messenger; however, the reasons
513 behind this essentiality have not been fully understood. In this study, we used the Gram-positive model
514 organism *B. subtilis* to gain further insights into the critical functions of c-di-AMP. Based on a variety
515 of distinct suppressor screens to adapt a *B. subtilis* strain lacking c-di-AMP to either the presence of
516 glutamate or to growth on complex medium, we can conclude that the control of potassium
517 homeostasis is the major bottleneck that limits growth of the mutant under both conditions. This is in
518 good agreement with (i) the large variety of c-di-AMP target proteins and RNA molecules that are
519 involved in the uptake and export of potassium in *B. subtilis* and other bacteria [11, 13, 20, 21, 23, 31,
520 34, 45, 78], (ii) the fact that the intracellular c-di-AMP levels seem to report the extracellular potassium
521 concentrations [18, 21, 37], and the isolation of suppressor mutants affecting potassium homeostasis
522 in response to altered cellular c-di-AMP levels also in other bacteria [18, 37]. However, our study also
523 clearly demonstrates that potassium is not the only problem for growth of *B. subtilis* in the absence of
524 c-di-AMP since the presence of mutations that reduce potassium uptake or facilitate its export is not
525 sufficient to overcome the toxicity of glutamate or complex medium. Suppressor studies with *L.*
526 *monocytogenes* and *S. aureus* mutants lacking c-di-AMP revealed that those mutants often had
527 acquired mutations in transporters for osmoprotectants such as glycine betaine indicating that
528 intoxication by compatible solutes is the main reason for essentiality of c-di-AMP in these latter
529 bacteria. The idea of a major role for c-di-AMP in osmoprotection rather than in potassium
530 homeostasis in these pathogenic bacteria is also supported by the observation that potassium has only
531 a minor impact on a *L. monocytogenes* strain lacking the only diadenylate cyclase [78]. Thus, while

532 general features of c-di-AMP signaling are conserved in different bacteria, the specific roles and
533 mechanisms may differ even between closely related bacteria.

534 Potassium and glutamate are the most abundant cation and anion, respectively, in every living
535 cell, and the intracellular concentrations of the two ions need to be balanced [79]. In *B. subtilis*, c-di-
536 AMP seems to play an important role in achieving this balance. The concentrations of the nucleotide
537 respond both to the potassium and the nitrogen source availability, they are high at high potassium
538 concentrations and in the presence of glutamate but not ammonium or glutamine [15, 21,40]. Our
539 work supports the idea of a close physiological integration of potassium and glutamate homeostasis:
540 Both potassium and glutamate inhibit growth of the Δ*dac* mutant independently of each other. The
541 accumulation of amino acids has also been shown to be a problem for the Δ*dac* mutants of *L.*
542 *monocytogenes* and *S. aureus*. As presented in this study, in both organisms amino acid transporters
543 were often inactivated in suppressor mutants that were capable of growing on complex medium
544 despite the lack of c-di-AMP: In *L. monocytogenes*, several suppressor mutants carried mutations
545 inactivating the OppABCD oligopeptide transporter [39] whereas the characterization of *S. aureus*
546 suppressor mutants resulted in the identification of the AlsT glutamine transporter, thus indicating
547 that glutamine rather than glutamate is toxic for the *S. aureus* Δ*dac* mutant [39, 42]. Again, these
548 differences between the related organisms support the idea that c-di-AMP has global overarching
549 functions in the different bacteria, but these can be put into practice differently.

550 It had been established previously that the accumulation of glutamate can be toxic for *B.*
551 *subtilis* [52, 80]. In the case of the Δ*dac* mutant, our work has unraveled three ways to overcome
552 glutamate toxicity: (i) Glutamate can be efficiently degraded upon decryptification of the otherwise
553 inactive *gudB* gene encoding the major constitutive glutamate dehydrogenase of *B. subtilis*. Such a
554 well established *gudB*$^+$ mutation [51] was found in the suppressor mutants GP2841 and GP3473. (ii)
555 The uptake of glutamate can be prevented, and this was indeed observed in many suppressor mutants.
556 Surprisingly, the recently characterized serine transporter AimA (YbeC) was identified as the main
557 glutamate transporter rather than the previsously studied GltT [73]. Even the Δ*dac* mutant lacking *gltT*

558 was unable to grow in the presence of glutamate unless AimA had been inactivated (see Fig. 1). This
559 observation as well as our detailed kinetic analyses revealed that AimA is the major low affinity
560 transporter for glutamate. Moreover, in the absence of c-di-AMP, the *aimA* gene is the most strongly
561 expressed gene encoding a glutamate transporter (see Fig. 5E). It is interesting to note that the
562 expression of *aimA* responds to the availability of c-di-AMP (see Fig. 5B), however, the mechanism
563 responsible for this control has yet to be uncovered. We have previously demonstrated that a
564 potassium channel (KtrCD) is directly activated and thus converted from a low- to a high-affinity uptake
565 system in the presence of glutamate [41]. Here, we show that similarly the affinity of the high affinity
566 glutamate transporter GltT is controlled by the presence of potassium: At high potassium
567 concentrations, the affinity of GltT for glutamate is increased fivefold. Thus, the uptake systems for
568 the two most abundant ions in the cell can respond to the presence of the other ion to keep their
569 intracellular concentrations balanced. (iii) In addition to mutations activating glutamate degradation
570 or preventing glutamate uptake, we found several mutants with paired mutations affecting lipid
571 biosynthesis and the mechanosensitive channel of small conductivity YfkC. Moreover, the Δ*dac yfkC**
572 mutant expressing the altered channel protein had to acquire additional mutations affecting either
573 glutamate uptake (*aimA*) or fatty acid biosynthesis (*accA*) to tolerate the otherwise toxic glutamate.
574 We suggest that the altered YfkC protein in conjunction with altered membrane properties facilitates
575 the export of glutamate. This idea is supported by the observation that YfkC needs a gain-of-function
576 mutation to bypass glutamate toxicity. Moreover, MscS-like mechanosensitive channels have been
577 shown to export glutamate in *Corynebacterium glutamicum* [81, 82]. In this bacterium, a gain of
578 function mutation affecting this channel results in constitutive glutamate secretion [83]. Finally,
579 specific membrane properties in *C. glutamicum* such as reduced lipid amounts facilitate glutamate
580 export by the MscS-like channel (see [84] for review). Our results and the parallels in *C. glutamicum*
581 strongly support the idea that the combination of mutations reducing lipid biosynthesis and that affect
582 the mechanosensitive channel YfkC allow glutamate export in *B. subtilis*, thus overcoming the toxic
583 effect of this amino acid.

584 Three lines of evidence suggest that respiration is a major bottleneck for *B. subtilis* in the
585 absence of c-di-AMP. First, many suppressors isolated in the presence of glutamate had mutations that
586 inactivate the *ndhF* gene encoding a subunit of a putative NADH dehydrogenase or the downstream
587 *ybcC* gene of unknown function. It is tempting to speculate that the two proteins form a complex that
588 catalyzes the oxidation of $NADH_2$. Second, when we used complex medium to isolate suppressor
589 mutants, this was initially only possible in the absence of oxygen if respiration activity was low. This is
590 paralleled by the observation that the *S. aureus* Δ*dac* is viable in the absence but not in the presence
591 of oxygen [40]. Finally, the lack of c-di-AMP results in an enhanced expression of the *ndhF-ybcC* operon
592 and reduced intracellular $NADH_2$ levels as indicated by the strong repression of the genes of the Rex
593 regulon in the Δ*dac* mutant. Although it is not yet understood how precisely respiration interferes with
594 the growth of the Δ*dac* mutant, it is tempting to speculate that the proton motive force generated by
595 respiration plays a key role: the major potassium transporter KimA is actually a proton:potassium
596 symporter [85],and potassium uptake by the KtrAB and KtrCD channels is directly driven by the proton
597 motive force [86]. Thus, a reduced respiration lowers the proton motive force and may thus limit the
598 uptake of potassium, the major growth-limiting factor for the *B. subtilis* Δ*dac* mutant.
599 The adaptation of the Δ*dac* mutant to complex medium did not only confirm the toxicity of
600 potassium, but it did also highlight the particular importance of the two c-di-AMP-binding signal
601 transduction proteins DarA and DarB. The acquisition of suppressor mutations that allow growth under
602 anaerobic conditions on complex medium was only possible when one of these proteins was absent
603 (see Fig. 1). This indicates that these proteins inhibit growth in their c-di-AMP-free apo form. For DarB
604 it has very recently been shown that the apo protein stimulates the synthesis of (p)ppGpp by the
605 alarmone synthetase Rel both in *B. subtilis* and *L. monocytogenes* [59, 60], and excessive (p)ppGpp
606 synthesis limits growth of both organisms [39, 59, 60]. For DarA, no function has been identified so far.
607 It is interesting to note, however, that DarA seems to be even more inhibitory than DarB since the Δ*dac*
608 Δ*darB* mutants tend to acquire additional mutations affecting DarA when adapting to the presence of
609 oxygen.

610 Taken together, our study supports the idea that c-di-AMP plays a central role in the physiology
611 of *B. subtilis*. Moreover, by comparing the results obtained with suppressor screens in closely related
612 but distinct bacteria, it becomes clear that the overall themes of c-di-AMP signaling are similar in
613 different bacteria whereas the precise mechanisms are not. While some of the functions of c-di-AMP
614 in *B. subtilis* such as the control of potassium homeostasis are already well understood, there remain
615 many open questions for future research such as the link between c-di-AMP and lipid biosynthesis and
616 the function of the PII-like signal transduction protein DarA. The work described here provides a solid
617 ground for further investigation.
618
619 **MATERIALS AND METHODS**
620
621 **Strains, media and growth conditions.** *E. coli* DH5α [87] was used for cloning and for the expression
622 of recombinant proteins. *E. coli* JM109 (Promega) was used for glutamate transporter
623 complementation assays. All *B. subtilis* strains used in this study are derivatives of the laboratory strain
624 168. They are listed in Table 2. *B. subtilis* was grown in Luria-Bertani (LB) or in sporulation (SP) medium
625 [87, 88]. For the assay of potassium and glutamate toxicity, *B. subtilis* was cultivated in MSSM medium
626 [21]. In this modified SM medium KH_2PO_4 was replaced by NaH_2PO_4 and KCl was added as indicated.
627 The media were supplemented with ampicillin (100 µg/ ml), kanamycin (10 and 50 µg/ ml for *B. subtilis*
628 and *E. coli*, respectively), chloramphenicol (5 µg/ ml), tetracyclin (12.5 µg/ ml), spectinomycin (150 µg/
629 ml) or erythromycin and lincomycin (2 and 25 µg/ ml, respectively) if required.
630
631 **Table 2.** Bacterial strains used in this study.

Strain	Genotype	Reference
168	*trpC2*	Laboratory collection
BKE14130	*trpC2 ΔdarB::erm*	[89]

GP94	*trpC2 ΔcdaA::spc*	[21]
GP342	*trpC2 amyE*::(*gltA-lacZ kan*)	[90]
GP987	*trpC2 ΔdisA::tet*	[9]
GP991	*trpC2 ΔcdaS::ermC ΔdisA::tet*	[9]
GP997	*trpC2 ΔcdaA::cat*	[9]
GP1360	*trpC2 ΔcdaS::spc*	This study
GP1361	*trpC2 ΔcdaS::spc disA::tet*	GP1360 → GP987
GP1712	*trpC2 ΔdarA::cat*	[47]
GP2181	*trpC2 amyE::*(P-*kimA*-RS-*lacZ cat*)	pGP2912 → 168
GP2222	*trpC2 ΔcdaA::cat ΔcdaS::ermC ΔdisA::tet*	[21]
GP2223	*trpC2 ΔcdaA::cat ΔcdaS::ermC ΔdisA::tet nhaK*$_{S187F}$	[21]
GP2224	*trpC2 ΔcdaA::cat ΔcdaS::ermC ΔdisA::tet aimA*$_{frameshift}$ *yqeG*$_{frameshift}$ *yqeV*$_{frameshift}$	This study
GP2245	*trpC2 ΔcdaS::ermC ΔdisA::tet ΔgltT::kan*	GP2248 → GP991
GP2248	*trpC2 ΔgltT::kan*	This study
GP2259	*trpC2 ΔcdaA::cat ΔcdaS::ermC ΔgltT::kan ΔdisA::tet*	GP997 → GP2245
GP2413	*trpC2 ΔcdaS::ermC ΔdisA::tet ΔdarA::cat*	GP1712 → GP991
GP2420	*trpC2 ΔcdaS::ermC ΔdisA::tet ΔdarA::cat ΔcdaA::spc*	GP94 → GP2413
GP2777	*trpC2 ΔcdaS::spc ΔdisA::tet ΔdarB::ermC*	BKE14130 → GP1361
GP2779	*trpC2 ΔcdaS::spc ΔdisA::tet ΔdarB::ermC ΔcdaA::cat*	GP997 → GP2777
GP2785	*trpC2 ΔyfkC::kan*	This study
GP2786	*trpC2 ΔaimA::kan*	This study
GP2796	*trpC2 ΔcdaS::spc disA::tet ΔyfkC::kan*	GP2785 → GP1361
GP2797	*trpC2 ΔcdaS::spc disA::tet ΔyfkC::kan ΔcdaA::cat*	GP997 → GP2796

GP2798	*trpC2 yfkC*$_{R42W}$ *kan*	This study
GP2813	*trpC2 ΔcdaS::spc disA::tet yfkC*$_{R42W}$ *kan*	GP2798 → GP1361
GP2814	*trpC2 ΔcdaS::spc disA::tet yfkC*$_{R42W}$ *kan ΔcdaA::cat*	GP997 → GP2813
GP2818	*trpC2 ΔgltP::cat ΔaimA::kan*	GP2786 → GP2824
GP2824	*trpC2 ΔgltP::cat*	This study
GP2825	*trpC2 ΔgltT::kan ΔgltP::cat*	GP2824 → GP2248
GP2831	*trpC2 ΔgltT::kan ΔaimA::phleo*	LFH → GP2248
GP2837	*trpC2 ΔcdaA::cat ΔcdaS::ermC ΔdisA::tet yfkC*$_{R42W}$ *plsC*$_{L48P}$ *fliP*$_{frameshift}$	This study
GP2838	*trpC2 ΔcdaA::cat ΔcdaS::ermC ΔdisA::tet ndhF*$_{V237E, M241L, H242L, A243D, G244C, L245F}$ *ΔydcL-yddM yoaI*$_{frameshift}$	This study
GP2839	*trpC2 ΔcdaA::cat ΔcdaS::ermC ΔdisA::tet fliK*$_{truncated}$ *rpoB*$_{Q109P}$ *rbsB*$_{R175L}$	This study
GP2840	*trpC2 ΔcdaA::cat ΔcdaS::ermC ΔdisA::tet plsC*$_{A61V}$ *ndhF*$_{frameshift}$ *ktrC*$_{frameshift}$ *sigD*$_{G88D}$	[41]
GP2841	*trpC2 ΔcdaA::cat ΔcdaS::ermC ΔdisA::tet gudB*$_{decrypt.}$ *accC*$_{H298Y}$	This study
GP2842	*trpC2 ΔcdaA::cat ΔcdaS::ermC ΔdisA::tet nhaK*$_{S187F}$ *aimA*$_{frameshift}$	This study
GP2845	*trpC2 ΔcdaS::spc ΔdisA::tet ΔdarB::ermC ΔcdaA::cat ktrC* (fs) *kimA*$_{Δ354-364}$ *darA*$_{V100A}$	This study
GP2849	*trpC2 ΔcdaA::cat ΔcdaS::ermC ΔdisA::tet aimA*$_{frameshift}$ *ybcC*$_{K722L/I724F}$	This study
GP2850	*trpC2 ΔcdaS::spc disA::tet yfkC*$_{R42W}$ *kan ΔcdaA::cat accA*$_{A229V}$ *yerC*$_{T58K}$ *ypoP*$_{KTEYF\ 111\ I}$	This study

GP3010	*trpC2 ΔcdaS::ermC ΔdisA::tet ΔdarA::cat ΔcdaA::spc* *ykoX*$_{K218STOP}$ *ktrC*$_{G11C}$ *yfkF*$_{G294S}$ *nusG*$_{T82K}$ *kimA*$_{\Delta G112}$ *ccpA*$_{\Delta bp850\text{-}1005}$ *(incl 24bp downstream)*	This study
GP3053	*trpC2 ΔcdaS::ermC ΔdisA::tet ΔaimA::phleo*	GP2831 → GP991
GP3054	*trpC2 ΔcdaS::ermC ΔdisA::tet ΔaimA::phleo ΔcdaA::cat*	GP997 → GP3053
GP3071	*trpC2 ΔgltT::kan ΔaimA::phleo ΔgltP::cat*	GP2824 → GP2831
GP3077	*trpC2 ΔcdaA::cat ΔcdaS::ermC ΔdisA::tet ktrC*$_{frameshift}$ *aimA/glpQ*$_{truncation}$ *ybcC*$_{frameshift}$	This study
GP3078	*trpC2 ΔcdaA::cat ΔcdaS::ermC ΔdisA::tet plsC*$_{A61V}$ *aimA*$_{T374M}$ *ktrB*$_{G313D}$ *sigD*$_{G88D}$	This study
GP3079	*trpC2 ΔcdaA::cat ΔcdaS::ermC ΔdisA::tet yfkC*$_{R42W}$ *plsC*$_{L48P}$ *Δ(abh-kinC-ykqA-ktrC) hbs*$_{I32T}$ *ndoA*$_{G6S}$ *fliP*$_{frameshift}$	This study
GP3093	*trpC2 ΔcdaA::cat ΔcdaS::ermC ΔgltT::kan ΔdisA::tet aimA*$_{L419P}$ *ndhF*$_{frameshift}$ *fliK*$_{frameshift}$	This study
GP3094	*trpC2 ΔcdaS::spc ΔdisA::tet ΔdarB::ermC ΔcdaA::cat* *ktrC*$_{frameshift}$ *kimA*$_{\Delta 354\text{-}364}$ *codY*$_{G146V}$ *yonD*$_{D255H}$	This study
GP3099	*trpC2 ΔcdaA::cat ΔcdaS::ermC ΔdisA::tet plsC*$_{L48P}$ *yfkC*$_{R42W}$ *fliP*$_{frameshift}$ *cotO*$_{I34F}$	This study
GP3101	*trpC2 ΔcdaS::ermC ΔdisA::tet ΔaimA::phleo ΔcdaA::cat* *fusA*$_{A579V}$ *yqeG*$_{frameshift}$	This study
GP3102	*trpC2 ΔcdaS::ermC ΔdisA::tet ΔaimA::phleo ΔcdaA::cat* *nhaK*$_{R486C}$ *sigA*$_{F281V}$ *mprA*$_{P397L}$ *fusA*$_{A579V}$	This study
GP3103	*trpC2 ΔcdaS::ermC ΔdisA::tet ΔaimA::phleo ΔcdaA::cat* *ktrC*$_{G14D}$ *topA*$_{K13N}$ *fusA*$_{A21T}$	This study

GP3105	*trpC2 ΔcdaS::spc disA::tet yfkC*$_{R42W}$ *kan ΔcdaA::cat aimA*$_{frameshift}$ *carB*$_{T257R}$ *mutL*$_{frameshift}$ *pksJ*$_{L4386F}$	This study
GP3464	*trpC2 ΔcdaA::cat ΔcdaS::ermC ΔdisA::tet plsC*$_{P110S}$ *flhA*$_{frameshift}$	This study
GP3473	*trpC2 ΔcdaA::cat ΔcdaS::ermC ΔdisA::tet ndhF*$_{frameshift}$ *aimA*$_{frameshift}$ *gudB*$^{+}$ *fliH*$_{frameshift}$ *yuiE*$_{G37V}$	This study
GP3474	*trpC2 ΔcdaA::cat ΔcdaS::ermC ΔdisA::tet ndhF* (fs) *aimA*$_{frameshift}$ *ykpA*$_{frameshift}$ *ktrC*$_{frameshift}$ *fliK*$_{frameshift}$ *fliH*$_{silent}$	This study
GP3486	*trpC2 ΔcdaA::cat ΔcdaS::ermC ΔdisA::tet nhaK*$_{S187F}$ *aimA*$_{frameshift}$	This study
GP3487	*trpC2 ΔcdaA::cat ΔcdaS::ermC ΔdisA::tet nhaK*$_{S187F}$ *aimA*$_{frameshift}$	This study
GP3488	*trpC2 ΔcdaA::cat ΔcdaS::ermC ΔdisA::tet nhaK*$_{S187F}$ *aimA*$_{frameshift}$	This study
GP3489	*trpC2 ΔcdaA::cat ΔcdaS::ermC ΔdisA::tet nhaK*$_{S187F}$ *aimA*$_{P279H}$	This study
GP3490	*trpC2 ΔcdaA::cat ΔcdaS::ermC ΔdisA::tet nhaK*$_{S187F}$ *aimA*$_{I164N}$	This study
GP3491	*trpC2 ΔcdaA::cat ΔcdaS::ermC ΔdisA::tet nhaK*$_{S187F}$ *aimA*$_{frameshift}$	This study
GP3492	*trpC2 ΔcdaA::cat ΔcdaS::ermC ΔdisA::tet nhaK*$_{S187F}$ *aimA*$_{frameshift}$	This study
GP3493	*trpC2 ΔcdaA::cat ΔcdaS::ermC ΔdisA::tet nhaK*$_{S187F}$ *aimA*$_{frameshift}$	This study
GP3494	*trpC2 ΔcdaA::cat ΔcdaS::ermC ΔdisA::tet nhaK*$_{S187F}$ *aimA*$_{S106P}$	This study
GP3495	*trpC2 ΔcdaA::cat ΔcdaS::ermC ΔdisA::tet nhaK*$_{S187F}$ *aimA*$_{N349K}$	This study
GP3496	*trpC2 ΔcdaA::cat ΔcdaS::ermC ΔdisA::tet nhaK*$_{S187F}$ *aimA*$_{frameshift}$	This study
GP3497	*trpC2 ΔcdaA::cat ΔcdaS::ermC ΔdisA::tet nhaK*$_{S187F}$ *aimA*$_{frameshift}$	This study
GP3498	*trpC2 ΔcdaA::cat ΔcdaS::ermC ΔdisA::tet nhaK*$_{S187F}$ *aimA*$_{G70R}$	This study
GP3499	*trpC2 ΔcdaA::cat ΔcdaS::ermC ΔdisA::tet nhaK*$_{S187F}$ *aimA*$_{Insertion\ after\ aa\ 226\ (+VA)}$	This study
GP3500	*trpC2 ΔcdaA::cat ΔcdaS::ermC ΔdisA::tet nhaK*$_{S187F}$ *aimA*$_{frameshift}$	This study
GP3701	*trpC2 ΔcdaA::cat ΔcdaS::ermC ΔdisA::tet nhaK*$_{S187F}$ *aimA*$_{frameshift}$	This study

GP3702	*trpC2 ΔcdaS::spc ΔdisA::tet ΔdarB::ermC ΔcdaA::cat* $ktrC_{frameshift}$ $kimA_{\Delta 354\text{-}364}$ $darA_{frameshift}$	This study
GP3703	*trpC2 ΔcdaS::spc ΔdisA::tet ΔdarB::ermC ΔcdaA::cat* $ktrC_{frameshift}$ $kimA_{\Delta 354\text{-}364}$ $darA_{frameshift}$	This study

632

633

634 **Suppressor screen**. For identification of suppressor mutations that rescue the growth of the c-di-AMP
635 lacking strain GP2222, a suppressor screen was set up. The same set-up was performed for the
636 suppressor screens with GP2223, GP2814, GP3054, and GP2259 (see Fig. 1). The respective strain was
637 plated on MSSM minimal plates in the presence of ammonium and 0.1 mM KCl. After incubation for
638 2-3 days, cell material was scraped from the plates and washed three times in MSSM basal salts
639 solution. These cells were either plated on MSSM minimal plates (Na-Glutamate, 0.1 mM KCl) or used
640 for inoculation of 10 ml MSSM minimal medium (Na-Glutamate, 0.1 mM KCl). The bacteria were then
641 incubated at 42°C for 3-4 days. As soon as suppressors appeared on the plates, they were picked and
642 re-isolated three times. For liquid cultures, as far as growth could be observed, they were plated.
643 Suppressors were picked and re-isolated again. For the suppressor screen on complex medium,
644 GP2222, GP2420, and GP2779 were plated on LB plates. The plates were incubated at 37°C either
645 under standard conditions (aerobic) or in an anaerobic jar to create an anaerobic environment. As soon
646 as suppressors appeared, they were picked and re-isolated three times. For the two step adaptation
647 to complex medium, suppressor mutants previously isolated in the anaerobic screen were plated on
648 LB plates and incubated at 37°C under aerobic conditions. As soon as new suppressors appeared, they
649 were picked and re-isolated three times. All isolated mutants were analyzed by whole-genome
650 sequencing (see below).

651

652 **Phenotypic characterization.** Amylase activity was detected on plates containing nutrient broth (7.5
653 g/liter), 17 g of Bacto agar per liter (Difco), and 5 g of hydrolyzed starch per liter (Connaught). The

654 ability to degrade starch was detected by sublimating iodine onto the plates. For quantitative
655 determination of *lacZ* expression in *B. subtilis,* cells were grown in MSSM medium with the nitrogen
656 source and potassium concentration as indicated and harvested in the exponential phase. β-
657 Galactosidase activity was determined with cell extracts obtained by lysozyme treatment as described
658 previously [88]. One unit of β-galactosidase is defined as the amount of enzyme that produces 1 nmol
659 of o-nitrophenol per minute at 28°C.

660 To assay growth of *B. subtilis* mutants at different potassium concentrations, the bacteria were
661 inoculated in LB medium and precultured in MSSM medium with 0.1 mM KCl. The cultures were grown
662 until exponential phase, harvested, washed three times in MSSM basal salts solution before the OD_{600}
663 was adjusted to 1.0. Dilution series were then pipetted onto MSSM plates with ammonium or
664 glutamate and 0.1 or 5 mM potassium.

665 Complementation in *E. coli* was assayed by transformation of strain JM109 that is unable to
666 grow with glutamate as the single source of carbon and nitrogen. For this purpose, the strain was
667 transformed with the complementation plasmid pGP2987 (*aimA*) and the empty vector control
668 pWH844. Growth of the transformants was assessed on M9 minimal medium plates containing either
669 ammonium and glucose or glutamate as carbon and nitrogen source [71].

670 **DNA manipulation and genome sequencing.** Transformation of *E. coli* and plasmid DNA extraction
671 were performed using standard procedures [87]. All commercially available plasmids, restriction
672 enzymes, T4 DNA ligase and DNA polymerases were used as recommended by the manufacturers.
673 Chromosomal DNA of *B. subtilis* was isolated as described [88]. *B. subtilis* was transformed with
674 plasmid and genomic DNA according to the two-step protocol [88].

675 To identify the mutations in the suppressor mutants, their genomic DNA was subjected to
676 whole-genome sequencing [91]. Briefly, the reads were mapped on the reference genome of *B. subtilis*
677 168 (GenBank accession number: NC_000964) [92] using the Geneious software package (Biomatters
678 Ltd., New Zealand) [93]. Single nucleotide polymorphisms were considered as significant when the

679 total coverage depth exceeded 25 reads with a variant frequency of ≥90%. All identified mutations
680 were verified by PCR amplification and Sanger sequencing.
681
682 **Construction of mutant strains by allelic replacement.** Gene deletion was achieved by transformation
683 of *B. subtilis* 168 with a PCR product constructed using oligonucleotides to amplify DNA fragments
684 flanking the target genes and an appropriate intervening resistance cassette as described previously
685 [94]. The mutation *yfkC*-R42W was introduced by amplification of regions containing and flanking the
686 mutation from strain GP2837, respectively, and a kanamycin resistance cassette was introduced
687 downstream of *yfkC* in the non-coding region between *yfkC* and *yfkD* (terminator region of both genes
688 present). The integrity of the regions flanking the integrated resistance cassette was verified by
689 sequencing PCR products of about 1,000 bp amplified from chromosomal DNA of the resulting mutant
690 strains.
691
692 **Plasmids.** Construction of a reporter fusion of the *kimA* promoter region with the promoterless *lacZ*
693 gene was done using the plasmid pAC6 [95]. The promoter fragment was cloned between the EcoRI
694 and BamHI sites of pAC6. The resulting plasmid was pGP2912. The plasmid was linearized with ScaI
695 and transformed into *B. subtilis* 168 for chromosomal integration into the *amyE* locus. For *E. coli*
696 complementation assays, the *aimA* gene was amplified using the primer pair LK167 (5'
697 AAAGGATCCATGAATCAATTGCATCGAAGAATGGGAACGTTTT)/ AK324 (5'
698 TTTGTCGACTTATTCTTTTCCGGCAGCAGCTTCTG) and cloned between the BamHI and SalI sites of the
699 expression vector pWH844 [72]. The resulting plasmid was pGP2987.
700
701 **Determination of apparent glutamate transporter kinetics**. The growth characteristics of *B. subtilis*
702 glutamate transporter mutants were used to determine the single glutamate transporter kinetics. The
703 mutants were either positive for *gltT* (*ΔgltP::cat ΔaimA::kan*) or *aimA* (*ΔgltT::kan ΔgltP::cat*) or lacked
704 both (*ΔgltT::kan ΔaimA::phleo ΔgltP::cat*). The nitrogen source was used as the limiting factor, so that

705 transport of glutamate was the essential factor for growth. The bacteria were inoculated in LB medium
706 and precultured in MSSM medium (ammonium) with 0.1/5 mM KCl. The cultures were grown until
707 exponential phase and the cells were washed three times in MSSM basal salts solution. Afterwards,
708 the cells were adjusted to OD_{600} 1.0 and used to inoculate a 96 well plate (Microtest Plate 96 Well, F,
709 Sarstedt) containing the MSSM medium with the respective glutamate and potassium concentrations.
710 The growth was tracked in an Epoch 2 Microplate Spectrophotometer (BioTek Instruments) at 37°C
711 with linear shaking at 237 cpm (4 mm) for 20 h, and optical density at 600 nm was measured in 10 min
712 intervals. The exponential growth phase was used to determine the growth rate μ [h^{-1}]. μ was
713 calculated from t_1 (early exponential phase) and t_2 (late exponential phase) and the corresponding OD_1
714 and OD_2 values. The resulting growth rates were then plotted against the glutamate concentrations.
715 This allowed fitting to the Monod equation and calculation of V_{max} [h^{-1}] and the apparent K_S [mM
716 glutamate] using the solver tool of Excel 2012 (Microsoft). Experiments were repeated with three
717 biological replicates.
718
719 **Transcriptome analysis.** Wild type and the c-di-AMP-deficient strains GP2222 Δ*dac* and GP2223 Δ*dac*
720 *nhaK*-S187F were grown in MSSM medium with ammonium or glutamate and low (0.1 mM) or high (5
721 mM) potassium concentrations. The strains were harvested by centrifugation (10.397 × g, 1 min, 4°C)
722 at mid exponential phase (OD_{600} of 0.4-0.6). A total of two independent biological replicates were
723 included. The pellets were frozen immediately in liquid nitrogen and stored at −80°C. Isolation of the
724 total RNA was done as described previously [96, 97], and the quality of the RNA preparations was
725 assessed by means of an Agilent 2100 Bioanalyzer according to the manufacturer's instructions. 5 µg
726 of total RNA were used for cDNA synthesis. The synthesis and fluorescence labeling of cDNA followed
727 a strand-specific method using the FairPlay III Microarray Labeling Kit (Agilent Technologies, Santa
728 Clara, CA, USA) and actinomycin D (Calbiochem) [98]. 200 ng of Cy3-labeled cDNA were hybridized to
729 the microarray following Agilent's hybridization, washing and scanning protocol (One-Color
730 Microarray-based Gene Expression Analysis, version 5.5). Data were extracted and processed using the

731 Feature Extraction software (version 11.5.1.1). An aggregated expression value was computed for each
732 annotated coding sequence and previously identified RNA feature [97]. Gene-level intensities were
733 scaled based on the intensity values of ten different *in vitro*-synthesized transcripts contained in the
734 One Color RNA Spike-In kit (Agilent Technologies) in order to account for technical variation associated
735 with sample processing. Genes with at least 2.5-fold difference in expression levels of the wild type at
736 the different conditions or between wild type and GP2222 mutant were considered significantly
737 affected.

738 To analyze the regulatory network, we compared the expression levels of the wild type strain
739 and the GP2222 mutant at ammonium 0.1 mM KCl. The genes were clustered in operons according to
740 their genetic localization, as described in *Subti*Wiki [99]. Additionally, gathered operons were grouped
741 by their corresponding documented regulator/s and metabolism. The visual representation of the
742 regulatory network was generated with Cytoscape and GIMP softwares [100, 101].

743

744 **Data availability statement.** The transcriptomic data reported in this study have been submitted to
745 the NCBI Gene Expression Omnibus (GEO; http://www.ncbi.nlm.nih.gov/geo/) under accession
746 number GSE156738.

747

748 **ACKNOWLEDGEMENTS**

749

750 We are grateful to Anika Klewing and Fabian Commichau for helpful discussion. We like to thank Felix
751 Mehne and Martin Weiss for the help with strain constructions and the initial characterization of a
752 suppressor mutant, respectively.

753

754

755 **REFERENCES**

756

757 1. Gomelsky M. cAMP, c-di-GMP, c-di-AMP, and now cGMP: bacteria use them all! Mol Microbiol.
758 2011; 79: 562-565.
759 2. Görke B, Stülke J. Carbon catabolite repression in bacteria: many ways to make the most out of
760 nutrients. Nat Rev Microbiol. 2008, 6: 613-624.
761 3. McDonough KA, Rodriguez A. The myriad roles of cyclic AMP in microbial pathogens: from signal
762 to sword. Nat Rev Microbiol. 2012; 10: 27-38.
763 4. Hengge R, Häussler S, Pruteanu M, Stülke J, Tschowri N, Turgay K. Recent advances and current
764 trends in nucleotide second messenger signaling in bacteria. J Mol Biol. 2019; 431: 908-927.
765 5. Jenal U, Reinders A, Lori C. Cyclic di-GMP: a second messenger extraordinaire. Nat Rev Microbiol.
766 2017; 15: 271-284.
767 6. Liu K, Bittner AN, Wang JD. Diversity in (p)ppGpp metabolism and effectors. Curr Opin Microbiol.
768 2015; 24: 72-79.
769 7. Hauryliuk V, Atkinson GC, Murakami KS, Tenson T, Gerdes K. Recent functional insights into the
770 role of (p)ppGpp in bacterial physiology. Nat Rev Microbiol. 2015; 13: 298-309.
771 8. Luo Y, Helmann JD. Analysis of the role of *Bacillus subtilis* σ^M in β-lactam resistance reveals an
772 essential role for c-di-AMP in peptidoglycan homeostasis. Mol Microbiol. 2012; 83: 623-639.
773 9. Mehne FM, Gunka K, Eilers H, Herzberg C, Kaever V, Stülke J. Cyclic di-AMP homeostasis in *Bacillus*
774 *subtilis*: both lack and high level accumulation of the nucleotide are detrimental for cell growth. J
775 Biol Chem. 2013; 288: 2004-2017.
776 10. Woodward JJ, Lavarone AT, Portnoy DA. c-di-AMP secreted by intracellular *Listeria*
777 *monocytogenes* activates a host type I interferon response. Science 2010; 328: 1703-1705.
778 11. Devaux L, Sleiman D, Mazzuoli MV, Gominet M, Lanotte P, Trieu-Cuot P, et al. Cyclic di-AMP
779 regulation of osmotic homeostasis is essential in group B *Streptococcus*. PLoS Genet. 2018; 14:
780 e1007342.

781 12. Corrigan RM, Bowman L, Willis AR, Kaever V, Gründling A. Cross-talk between two nucleotide-
782 signaling pathways in *Staphylococcus aureus*. J Biol Chem. 2015; 290: 5826-5839.
783 13. Blötz C, Treffon K, Kaever V, Schwede F, Hammer E, Stülke J. Identification of the components
784 involved in cyclic di-AMP signaling in *Mycoplasma pneumoniae*. Front Microbiol. 2017; 8: 1328.
785 14. Barker JR, Koestler BJ, Carpenter VK, Burdette DL, Waters CM, et al. STING-dependent recognition
786 of cyclic di-AMP mediates type I interferon responses during *Chlamydia trachomatis* infection.
787 mBio 2013; 4: e00018-13.
788 15. Gundlach J, Mehne FMP, Herzberg C, Kampf J, Valerius O, Kaever V, Stülke J. An essential poison:
789 synthesis and degradation of cyclic di-AMP in *Bacillus subtilis*. J Bacteriol. 2015; 197: 3265-3274.
790 16. Smith WM, Pham TH, Lei L, Dou J, Soomro AH, et al. Heat resistance and salt hypersensitivity in
791 *Lactococcus lactis* due to spontaneous mutation in llmg1816 (*gdpP*) induced by high-temperature
792 growth. Appl Environ Microbiol. 2012; 78: 7753-7759.
793 17. Huynh TN, Luo S, Pensinger D, Sauer JD, Tong L, Woodward JJ. An HD-domain phosphodiesterase
794 mediates cooperative hydrolysis of c-di-AMP to affect bacterial growth and virulence. Proc Natl
795 Acad Sci USA. 2015; 112: E747-E756.
796 18. Zarrella TM, Metzger DW, Bai G. Stress suppressor screening leads to detecting regulation of cyclic
797 di-AMP homeostasis by a Trk-family effector protein in *Streptococcus pneumoniae*. 2018; J
798 Bacteriol. 200: e00045-18.
799 19. Zhu Y, Pham TH, Nhiep TH, Vu NM, Marcellin E, et al. Cyclic-di-AMP synthesis by the diadenylate
800 cyclase CdaA is modulated by the peptidoglycan biosynthesis enzyme GlmM in *Lactococcus lactis*.
801 Mol Microbiol. 2016; 99: 1015-1027.
802 20. Nelson JW, Sudarsan N, Furukawa K, Weingerg Z, Wang JX, Breaker RR. Riboswitches in eubacteria
803 sense the second messenger cyclic di-AMP. Nat Chem Biol. 2013; 9: 834-839.
804 21. Gundlach J, Herzberg C, Kaever V, Gunka K, Hoffmann T, Weiß M, et al. Control of potassium
805 homeostasis is an essential function of the second messenger cyclic di-AMP in *Bacillus subtilis*. Sci
806 Signal. 2017; 10: eaal3011.

807 22. Gundlach J, Herzberg C, Hertel D, Thürmer A, Daniel R, Link H, Stülke J. Adaptation of *Bacillus*
808 *subtilis* to life at extreme potassium limitation. mBio 2017; 8: e00861-17.
809 23. Gundlach J, Krüger L, Herzberg C, Turdiev A, Poehlein A, Tascón I, et al. Sustained sensing in
810 potassium homeostasis: Cyclic di-AMP controls potassium uptake by KimA at the levels of
811 expression and activity. J Biol Chem. 2019; 294: 9605-9614.
812 24. Hutchison CA, Peterson SN, Gill SR, Cline RT, White O, Fraser CM, et al. Global transposon
813 mutagenesis and a minimal Mycoplasma genome. Science 1999; 286: 2165-2169.
814 25. Commichau FM, Pietack N, Stülke J. Essential genes in *Bacillus subtilis*: A re-evaluation after ten
815 years. Mol Biosyst. 2013; 9: 1068-1075.
816 26. Rancati G, Moffat J, Typas A, Pvelka N. Emerging and evolving concepts in gene essentiality. Nat
817 Rev Genet. 2018; 19: 34-49.
818 27. Reuß DR, Faßhauer P, Mroch PJ, Ul-Haq I, Koo BM, Pöhlein A, et al. Topoisomerase IV can
819 functionally replace all type 1A topoisomerases in *Bacillus subtilis.* Nucleic Acids Res. 2019; 47:
820 5231-5242.
821 28. Benda M, Woelfel S, Gunka K, Klumpp S, Poehlein A, Kálalová D, et al. Quasi-essentiality of RNase
822 Y in *Bacillus subtilis* is caused by its critical role in the control of mRNA homeostasis. doi:
823 https://doi.org/10.1101/2020.05.20.106237.
824 29. Tödter D, Gunka K, Stülke J. The highly conserved Asp23 family protein YqhY plays a role in lipid
825 biosynthesis in *Bacillus subtilis*. Front Microbiol. 2017; 8: 883.
826 30. Gallagher LA, Bailey J, Manoil C. Ranking essential bacterial processes by speed of mutant death.
827 Proc Natl Acad Sci USA. 2020; 117: 18010-18017.
828 31. Corrigan RM, Campeotto I, Jeganathan T, Roelofs KG, Lee VT, Gründling A. Systematic
829 identification of conserved bacterial c-di-AMP receptor proteins. Proc Natl Acad Sci USA. 2013;
830 110: 9084-9089.
831 32. Huynh TN, Choi PH, Sureka K, Ledvina HE, Campillo J, et al. Cyclic di-AMP targets the cystathione
832 beta-synthase domain of the osmolyte transporter OpuC. Mol Microbiol. 2016; 102: 233-243.

833 33. Schuster CF, Bellows LE, Tosi T, Campeotto I, Corrigan RM, et al. The second messenger c-di-AMP
834 inhibits the osmolyte uptake system OpuC in *Staphylococcus aureus*. Sci Signal. 2016; 9: ra81.
835 34. Quintana IM, Gibhardt J, Turdiev A, Hammer E, Commichau FM, et al. The KupA and KupB proteins
836 of *Lactococcus lactis* IL1403 are novel c-di-AMP receptor proteins responsible for potassium
837 uptake. J Bacteriol. 2019; 201: e00028-19.
838 35. Latoscha A, Drexler DJ, Al-Bassam MM, Kaever V, Findlay KC, et al. 2020. C-di-AMP hydrolysis by
839 a novel type of phosphodiesterase promotes differentiation of multicellular bacteria. Proc Natl
840 Acad Sci USA. 2020; 117: 7392-7400.
841 36. Moscoso JA, Schramke H, Zhang Y, Tosi T, Dehbi A, et al. Binding of cyclic di-AMP to the
842 *Staphylococcus aureus* sensor kinase KdpD occurs via the Universal Stress Protein domain and
843 downregulates the expression of the Kdp potassium transporter. J Bacteriol. 2015; 198: 98-110.
844 37. Pham HT, Nhiep NTH, Vu TNM, Huynh TN, Zhu Y, et al. Enhanced uptake of potassium or glycine
845 betaine or export of cyclic di-AMP restores osmoresistance in a high cyclic-di-AMP *Lactococcus*
846 *lactis* mutant. PLoS Genet. 2018; 14: e1007574.
847 38. Rubin BE, Huynh TN, Welkie DG, Diamond S, Simkovsky R, et al. High-throughput interaction
848 screens illuminate the role of c-di-AMP in cyanobacterial nighttime survival. PLoS Genet. 2018;
849 14: e1007301.
850 39. Whiteley AT, Pollock AJ, Portnoy DA. The PAMP c-di-AMP is essential for *Listeria monocytogenes*
851 growth in macrophages and rich but not minimal medium due to a toxic increase in (p)ppGpp. Cell
852 Host Microbe 2015; 17: 788-798.
853 40. Zeden MS, Schuster CF, Bowman L, Zhong Q, Williams HD, Gründling A. Cyclic di-adenosine
854 monophosphate (c-di-AMP) is required for osmotic regulation in *Staphylococcus aureus* but
855 dispensable for viability in anaerobic conditions. J. Biol. Chem. 2018; 293: 3180-3200.
856 41. Krüger L, Herzberg C, Warneke R, Poehlein A, Stautz J, Weiß M, et al. Two ways to convert a low-
857 affinity potassium channel to high affinity: Control of *Bacillus subtilis* KtrCD by glutamate. J.
858 Bacteriol. 2020; 202: e00138-20.

859 42. Zeden MS, Kviatkovski I, Schuster CF, Thomas VC, Fey PD, Gründling A. Identification of the main
860 glutamine and glutamate transporters in *Staphylococcus aureus* and their impact on c-di-AMP
861 production. Mol Microbiol. 2020; 113: 1085-1100.
862 43. Commichau FM, Gibhardt J, Halbedel S, Gundlach J, Stülke J. 2018. A delicate connection: c-di-
863 AMP affects cell integrity by controlling osmolyte transport. Trends Microbiol. 26:175-185.
864 44. He J, Yin W, Galperin MY, Chou SH. Cyclic di-AMP, a second messenger of primary importance:
865 tertiary structures and binding mechanisms. Nucleic Acids Res. 2020; 48: 2807-2829.
866 45. Stülke J, Krüger L. Cyclic di-AMP signaling in bacteria. Annu Rev Microbiol. 2020; 74: 159-179.
867 46. Mehne FMP, Schröder-Tittmann K, Eijlander RT, Herzberg C, Hewitt L, et al. Control of the
868 diadenylate cyclase CdaS in *Bacillus subtilis*: An autoinhibitory domain limits c-di-AMP production.
869 J Biol Chem. 2014; 289: 21098-21107.
870 47. Gundlach J, Dickmanns A, Schröder-Tittmann K, Neumann P, Kaesler J, Kampf J, et al.
871 Identification, characterization and structure analysis of the c-di-AMP binding P_{II}-like signal
872 transduction protein DarA. J Biol Chem. 2015; 290: 3069-3080.
873 48. Rosenberg J, Müller P, Lentes S, Thiele MJ, Zeigler DR, Tödter D, et al. ThrR, a DNA-binding
874 transcription factor involved in controlling threonine biosynthesis in *Bacillus subtilis*. Mol.
875 Microbiol. 2016; 101: 879-893.
876 49. Reuß DR, Rath H, Thürmer A, Benda M, Daniel R, Völker U, et al. Changes of DNA topology affect
877 the global transcription landscape and allow rapid growth of a *Bacillus subtilis* mutant lacking
878 carbon catabolite repression. Metab. Eng. 2018; 45: 171-179.
879 50. Kampf J, Gerwig J, Kruse K, Cleverley R, Dormeyer M, Grünberger A, et al. Selective pressure for
880 biofilm formation in *Bacillus subtilis*: differential effect of mutations in the master regulator SinR
881 on bistability. mBio 2018; 9: e00166-18.
882 51. Belitsky BR, Sonenshein AL. Role and regulation of *Bacillus subtilis* glutamate dehydrogenase
883 genes. J Bacteriol. 1998; 180: 6298-6305.

884 52. Commichau FM, Gunka K, Landmann JJ, Stülke J. Glutamate metabolism in *Bacillus subtilis*: Gene
885 expression and enzyme activities evolved to avoid futile cycles and to allow rapid responses to
886 perturbations in the system. J Bacteriol. 2008; 190:3557-3564.
887 53. Klewing A, Koo BM, Krüger L, Poehlein A, Reuß D, Daniel R, et al. Resistance to serine in *Bacillus*
888 *subtilis*: identification of the serine transporter YbeC and of a metabolic network that links serine
889 and threonine metabolism. Environ. Microbiol. 2020; in press. doi: https://doi.org/10.1111/1462-
890 2920.15179.
891 54. Calvo RA, Kearns DB. FlgM is secreted by the flagellar export apparatus in *Bacillus subtilis*. J
892 Bacteriol. 2015; 197:8-91.
893 55. Wahome PG, Setlow P. Growth, osmotic downshock resistance and differentiation of *Bacillus*
894 *subtilis* lacking mechanosensitive channels. Arch Microbiol. 2008; 189: 49-58.
895 56. Hoffmann T, Boiangiu C, Moses S, Bremer E. Responses of *Bacillus subtilis* to hypotonic challenges:
896 physiological contributions of mechanosensitive channels to cellular survival. Appl Environ
897 Microbiol. 2008; 74: 2454-2460.
898 57. Kempf B, Bremer E. OpuA, an osmolytically regulated binding protein-dependent transport
899 system for the osmoprotectant glycine betaine in *Bacillus subtilis*. J Biol Chem. 1995; 270: 16701-
900 16713.
901 58. Tascón I, Sousa JS, Corey RA, Mills DJ, Griwatz D, Aumüller N, et al. Structural basis of proton-
902 coupled potassium transport in the KUP family. Nat Commun. 2020; 11: 626.
903 59. Krüger L, Herzberg C, Wicke D, Bähre H, Heidemann JL, Dickmanns, et al. A rendezvous of two
904 second messengers: The c-di-AMP receptor protein DarB controls (p)ppGpp synthesis in *Bacillus*
905 *subtilis*. https://doi.org/10.1101/2020.08.27.268672.
906 60. Peterson BN, Young MKM, Lou S, Wang J, Whiteley AT, Woodward JJ, et al. (p)ppGpp and c-di-
907 AMP homeostasis is controlled by CbpB in *Listeria monocytogenes*. mBio 2020; 11: e01625-20.
908 61. Larsson JT, Rogstam A, von Wachenfeldt C. Coordinated patterns of cytochrome bd and lactate
909 dehydrogenase expression in *Bacillus subtilis*. Microbiology 2005; 151: 3323-3335.

910 62. Gyan S, Shiohira Y, Sato I, Takeuchi M, Sato T. Regulatory loop between redox sensing of the
911 NADH/NAD$^+$ ratio by Rex (YdiH) and oxidation of NADH by NADH dehydrogenase Ndh in *Bacillus*
912 *subtilis*. J Bacteriol. 2006; 188: 7062-7071.
913 63. Qi Y, He Y, She Q, Larese-Casanova P, Li P, Chai Y. Heterogeneity in respiratory electron transfer
914 and adaptive iron utilization in a bacterial biofilm. Nat Commun. 2019; 10: 3702.
915 64. MacLellan SR, Wecke T, Helmann JD. A previously unidentified σ factor and two accessory proteins
916 regulate oxalate decarboxylase expression in *Bacillus subtilis*. Mol Microbiol. 2008; 69: 954-967.
917 65. Zhang X, Wang J, Feng Y, Ge J, Li W, Sun W, et al. Structure and molecular mechanism of an anion-
918 selective mechanosensitive channel of small conductance. Proc Natl Acad Sci USA. 2012; 109:
919 18180-18185.
920 66. Bilder P, Lightle S, Bainbridge G, Ohren J, Finzel B, Sun F, et al. The structure of the
921 carboxyltransferase component of acetyl-CoA carboxylase reveals a zinc-binding motif unique to
922 the bacterial enzyme. Biochemistry 2006; 45: 1712-1722.
923 67. Silvers MA, Pakhomova S, Neau DB, Silvers WC, Anzalone N, Taylor CM, Waldrop GL. Crystal
924 structure of carboxyltransferase from *Staphylococcus aureus* bound to the antibacterial agent
925 moiramide B. Biochemistry 2016; 55: 4666-4674.
926 68. Robertson RM, Yao J, Gajewski S, Kumar G, Martin EW, Rock CO, White SW. A two-helix motif
927 positions the lysophatidic acid acyltransferase active site for catalysis within the membrane
928 bilayer. Nat Struct Mol Biol 2017; 24: 666-671.
929 69. Pliotas C, Dahl ACE, Rasmussen T, Mahendran KR, Smith TK, Marius P, et al. The role of lipids in
930 mechanosensation. Nat Struct Mol Biol. 2015; 22: 991-998.
931 70. Rasmussen T, Rasmussen A, Yang L, Kaul C, Black S, Galbiati, et al. Interaction of the
932 mechanosensitive channel, MscS, with the membrane bilayer through lipid intercalation into
933 grooves and pockets. J Mol Biol. 2019; 431: 3339-3352.
934 71. Halpern YS, Lupo M. Glutamate transport in wild-type and mutant strains of *Escherichia coli*. J
935 Bacteriol. 1965; 90: 1289-1295.

936 72. Schirmer F, Ehrt S, Hillen W. Expression, inducer spectrum, domain structure, and function of
937 MopR, the regulator of phenol degradation in *Acinetobacter calcoaceticus* NCIB8250. J Bacteriol.
938 1997; 179: 1329-1336.
939 73. Zaprasis A, Bleisteiner M, Kerres A, Hoffmann T, Bremer E. Uptake of amino acids and their
940 metabolic conversion into the compatible solute proline confers osmoprotection to *Bacillus*
941 *subtilis*. Appl Environ Microbiol. 2015; 81: 250-259.
942 74. Liu G, Song G, Zhang D, Zhang D, Li Z, Lyu Z, et al. EF-G catalyzes tRNA translocation by disrupting
943 interactions between decoding center and codon-anticodon duplex. Nat Struct Mol Biol. 2014; 21:
944 817-824.
945 75. Peng BZ, Bock LV, Belardinelli, Peske F, Grubmüller H, Rodnina MV. Active role of elongation factor
946 G in maintaining the mRNA reading frame during translation. Sci Adv. 2019; 5: eaax8030.
947 76. Maracci C, Peske F, Dannies E, Pohl C, Rodnina MV. Ribosome-induced tuning of GTP hydrolysis
948 by a translational GTPase. Proc Natl Acad Sci USA. 2014; 111: 14418-14423.
949 77. Terakawa A, Natsume A, Okada A, Nishihata S, Kuse J, Tanaka K, et al. *Bacillus subtilis* 5'-
950 nucleotidases with various functions and substrate specificities. BMC Microbiol. 2016; 16: 249.
951 78. Gibhardt J, Hoffmann G, Turdiev A, Wang M, Lee VT, Commichau FM. C-di-AMP assists
952 osmoadaptation by regulating the *Listeria monocytogenes* potassium transporters KimA and
953 KtrCD. J Biol Chem. 2019; 294: 16020-16033.
954 79. Gundlach J, Commichau FM, Stülke J. Of ions and messengers: an intricate link between potassium,
955 glutamate and cyclic di-AMP. Curr Genet. 2018; 64:191-195.
956 80. Gunka K, Tholen S, Gerwig J, Herzberg C, Stülke J, Commichau FM. A high-frequency mutation in
957 *Bacillus subtilis*: requirements for the decryptification of the *gudB* glutamate dehydrogenase gene.
958 J Bacteriol. 2012; 194: 1036-1044.
959 81. Becker M, Börngen K, Nomura T, Battle AR, Marin K, et al. Glutamate efflux mediated by
960 *Corynebacterium glutamicum* MscCG, *Escherichia coli* MscS, and their derivatives. Biochim Biohys
961 Acta. 2013; 1828:1230-1240.

962 82. Wang Y, Cao G, Xu D, Fan L, Wu X, Ni X, et al. A novel *Corynebacterium glutamicum* L-glutamate
963 exporter. Appl Environ Microbiol. 2018; 84:e02691-17.
964 83. Nakayama Y, Yoshimura K, Iida H. A gain-of-function mutation in gating of *Corynebacterium*
965 *glutamicum* NCgl1221 causes constitutive glutamate secretion. Appl Environ Microbiol. 2012;
966 78:5432-5434.
967 84. Nakayama Y,Hashimoto KI, Kawasaki H, Martinec B. "Force-From-Lipids" mechanosensation in
968 *Corynebacterium glutamicum*. Biophys Rev. 2019; 11:327-333.
969 85. Tascon I, Sousa JS, Corey RA, Mills DJ, Griwatz D, et al. Structural basis of proton coupled
970 potassium transport in the KUP family. Nat Commun. 2020; 11:626.
971 86. Diskowski M, Mikusevic V, Stock C, Hänelt I. 2015. Functional diversity of the superfamily of K^+
972 transporters to meet various requirements. Biol. Chem. 396:1003-1014.
973 87. Sambrook J, Russell D. 2001. Molecular Cloning: A Laboratory Manual, Cold Spring Harbor
974 Laboratory, Cold Spring Harbor.
975 88. Kunst F, Rapoport G. Salt stress is an environmental signal affecting degradative enzyme synthesis
976 in *Bacillus subtilis*. J Bacteriol. 1995; 177:2403-2407.
977 89. Koo BM, Kritikos G, Farelli JD, Todor H, Tong K, Kimsey H, et al. Construction and analysis of two
978 genome-scale deletion libraries for *Bacillus subtilis*. Cell Syst. 2017; 4: 291-305.
979 90. Wacker I, Ludwig H, Reif I, Blencke HM, Detsch C, Stülke J. The regulatory link between carbon
980 and nitrogen metabolism in *Bacillus subtilis*: regulation of the *gltAB* operon by the catabolite
981 control protein CcpA. Microbiology. 2003; 149: 3001-3009.
982 91. Reuß DR, Altenbuchner J, Mäder U, Rath H, Ischebeck T, Sappa PK, et al. Large-scale reduction of
983 the *Bacillus subtilis* genome: consequences for the transcriptional network, resource allocation,
984 and metabolism. Genome Res. 2017; 27:289-299.
985 92. Barbe V, Cruveiller S, Kunst F, Lenoble P, Meurice G, Sekowska A, et al. From a consortium
986 sequence to a unified sequence: the *Bacillus subtilis* 168 reference genome a decade later.
987 Microbiology 2009; 155:1758-1775.

988 93. Kearse M, Moir R, Wilson A, Stones-Havas S, Cheung M, Sturrock S, et al. Geneious basic: an
989 integrated and extendable desktop software platform for the organization and analysis of
990 sequence data. Bioinformatics 2012; 28:1647–1649.
991 94. Diethmaier C, Pietack N, Gunka K, Wrede C, Lehnik-Habrink M, Herzberg C, et al. A novel factor
992 controlling bistability in *Bacillus subtilis*: the YmdB protein affects flagellin expression and biofilm
993 formation. J Bacteriol. 2011; 193: 5997-6007.
994 95. Stülke J, Martin-Verstraete I, Zagorec M, Rose M, Klier A, Rapoport G. Induction of the *Bacillus*
995 *subtilis ptsGHI* operon by glucose is controlled by a novel antiterminator, GlcT. Mol Microbiol.
996 1997; 25: 65-78.
997 96. Eymann C, Homuth G, Scharf C, Hecker M. *Bacillus subtilis* functional genomics: global
998 characterization of the stringent response by proteome and transcriptome analysis. J Bacteriol.
999 2002; 184: 2500-2520.
1000 97. Nicolas P, Mäder U, Dervyn E, Rochat T, Leduc A, Pigeonneau N, et al. Condition-dependent
1001 transcriptome reveals high-level regulatory architecture in *Bacillus subtilis*. Science 2012; 335:
1002 1103-1106.
1003 98. Mäder U, Nicolas P. Array-based approaches to bacterial transcriptome analysis. In Methods in
1004 Microbiology, Vol. 39, eds. C. Harwood, A. Wipat (Cambridge Academic Press), 151-182.
1005 99. Zhu B, Stülke J. *Subti*Wiki in 2018: from genes and proteins to functional network annotation of
1006 the model organism *Bacillus subtilis*. Nucleic Acids Res. 2018; 46: D743-D748.
1007 100. Shannon P, Markiel A, Ozier O, Baliga NS, Wang JT, Ramage D, et al. Cytoscape: a software
1008 environment for integrated models of biomolecular interaction networks. Genome Res. 2003; 13:
1009 2498-504.
1010 101. The GIMP Development Team. GIMP. 2019; Retrieved from https://www.gimp.org.
1011

1012 **SUPPORTING INFORMATION CAPTIONS**

1013

1014 **S1 Supporting Information**

1015 Global gene expression in the *B. subtilis* wild type strain in response to the potassium concentration

1016 and the nitrogen source.

1017

1018 **S1 Table**

1019 Transcriptomic data for the genes that are most strongly affected by the absence of c-di-AMP (Ammonium

1020 0.1 mM KCl).

1021

1022 **S2 Table.**

1023 Transcriptomic data of genes involved in c-di-AMP, potassium, and glutamate homeostasis.

1024

1025 **S1 Fig. Acquisition of beneficial mutations allows growth of a c-di-AMP deficient strain in the**

1026 **presence of glutamate.**

1027 Growth assay of *B. subtilis* wild type, GP2222 (Δ*dac*), and the isolated glutamate suppressor mutants.

1028 *B. subtilis* strains were cultivated in MSSM minimal medium with 0.1 mM KCl and ammonium. The cells

1029 were harvested, washed, and the OD_{600} was adjusted to 1.0. Serial dilutions were dropped onto MSSM

1030 minimal plates with the indicated potassium concentration and ammonium or glutamate, or on LB

1031 plates.

1032

1033 **S2 Fig. Potassium and glutamate influenced promoters.**

1034 The expression of the high-affinity potassium transporter *kimA* (A) and the glutamate synthase *gltA* (B)

1035 was assessed by fusion of the promoter to the reporter gene *lacZ*. The cells harboring the promoter-

1036 fusion were cultivated with ammonium or glutamate at 0.1 mM KCl (*kimA*) or ammonium and different

1037 potassium concentrations (0.1, 5, 20 mM; *gltA*). Promoter activity was analyzed by quantification of β-

1038 galactosidase activity. Statistical analysis was performed using a one-way ANOVA, followed by Tukey's
1039 multiple comparisons test (**** $P < 0.0001$).
1040
1041 **S3 Fig. Two-step adaptation to complex medium.**
1042 Growth assay of *B. subtilis* wild type, GP2779 (Δ*dac* Δ*darB*), GP2420 (Δ*dac* Δ*darA*) and the isolated
1043 glutamate suppressor mutants. *B. subtilis* strains were precultivated in LB medium. The cells were
1044 harvested, washed, and the OD_{600} was adjusted to 1.0. Serial dilutions were dropped onto MSSM
1045 minimal plates with 0.1 mM KCl and ammonium or on LB plates.
1046
1047 **S4 Fig. Mutations in the mechanosensitive channel YfkC.** Mutations in the *yfkC* gene were obtained
1048 in the suppressor screen with glutamate (Table 1). The amino acid substitution Arg42 to Trp was
1049 observed in three independently isolated clones. In *E. coli* localization of S58 was observed to be highly
1050 dependent on the closing state of the channel (Miller *et al*., 2003), thus, it appears likely that amino
1051 acid residue 42 in *B. subtilis* is located close to the gate.
1052
1053 **S5 Fig. Mutations in the acetyl-CoA carboxylase subunits.**
1054 Mutations obtained in the suppressor screen with glutamate (Table 1) and LB (Table 4). All mutations
1055 were single amino acid substitutions from independently isolated clones. Both mutations are located
1056 in highly conserved regions of AccA and AccC (hatched boxes) close to the active center.
1057
1058 **S6 Fig. Mutations in the acyl-ACP:1-acylglycerolphosphate acyltransferase.** Mutations in the *plsC*
1059 gene were obtained in the suppressor screen with glutamate (Table 1). All mutations were single amino
1060 acid substitutions from independently isolated clones. All mutations are located in functionally
1061 important regions of the enzyme.
1062
1063

1064 **S7 Fig. Mutations in the elongation factor G (FusA).** Mutations in the *fusA* gene were obtained in the
1065 suppressor screen of GP3054 (Δ*dac* Δ*aimA*) with glutamate (Table 3). The amino acid substitution
1066 Ala21 to Thr was observed in one suppressor. Ala21 is adjacent to Asp20, an amino acid residue that
1067 binds the Mg ion and is therefore crucial for GTPase activity of the protein (Maracci *et al*., 2014). In the
1068 two other suppressors Ala579 was mutated to Val. This amino acid residue is located in the conserved
1069 loop II that is required for proper translocation (Peng *et al*., 2019).
1070
1071 **S8 Fig. Effect of the deletion of the glutamate transporters in a c-di-AMP deficient strain.**
1072 Growth assay of *B. subtilis* wild type, GP2222 (Δ*dac*), GP3054 (Δ*dac* Δ*aimA*), GP2248 (Δ*dac* Δ*gltT*) and
1073 the isolated glutamate suppressor mutants. *B. subtilis* strains were cultivated in MSSM minimal
1074 medium with 0.1 mM KCl and ammonium. The cells were harvested, washed, and the OD_{600} was
1075 adjusted to 1.0. Serial dilutions were dropped onto MSSM minimal plates with the indicated potassium
1076 concentration and ammonium or glutamate, or on LB plates.
1077

1078 **Figure legends**

1079

1080 **Fig. 1. A suppressor screen with a strain lacking c-di-AMP reveals the complexity of glutamate**
1081 **toxicity.**

1082 GP2222 (Δ*dac*), GP2814 (Δ*dac yfkC**), GP2223 (Δ*dac nhaK**), GP2259 (Δ*dac* Δ*gltT*), and GP3054 (Δ*dac*
1083 Δ*aimA*) were cultivated in MSSM medium with glutamate and 0.1 mM KCl and suppressors were
1084 isolated and analyzed by whole genome sequencing. Note that for GP2222 (Δ*dac*), 14 mutants were
1085 isolated in this study and one mutant was isolated previously [41] but studied in depth here, thus
1086 resulting in a total number of 15 mutants.

1087

1088 **Fig. 2. A suppressor screen with a strain lacking c-di-AMP on complex medium.**

1089 GP2222 (Δ*dac*), GP2420 (Δ*dac* Δ*darA*), or GP2779 (Δ*dac* Δ*darB*) were cultivated on LB agar plates and
1090 incubated under aerobic or anaerobic conditions as indicated. The table shows how the parental strain
1091 evolved, and under which conditions suppressors could be isolated. The suppressor mutants were
1092 analyzed by whole genome sequencing.

1093

1094 **Fig. 3. Regulatory network of the most strongly up- and downregulated genes as a result of the lack**
1095 **of c-di-AMP.**

1096 Expression ratios of *B. subtilis* wild type and GP2222 (Δ*dac*) with ammonium and 0.1 mM KCl were
1097 calculated and the most up- or downregulated genes were clustered into operons, regulons, and
1098 grouped depending on their physiological function. Regulators are depicted as large blue nodes, and
1099 regulated operons or genes as yellow and orange nodes for up- and downregulated genes,
1100 respectively). Arrows: green: activation; gray: sigma-factor; red: repression.

1101

1102 **Fig. 4. The influence of the mechanosensitive channel YfkC on growth of a *B. subtilis* strain lacking c-**
1103 **di-AMP in the presence of glutamate.**

1104 *B. subtilis* strains were cultivated in MSSM minimal medium with 0.1 mM KCl and glutamate. Cells were
1105 harvested, washed, and the OD_{600} was adjusted to 1.0. Serial dilutions were dropped onto MSSM
1106 minimal plates with the indicated potassium concentration and ammonium or glutamate, or on LB
1107 plates.
1108
1109 **Fig. 5. Identification of AimA as a novel low-affinity glutamate transporter.**
1110 (A) *E. coli* JM109 was transformed with pGP2987 (AimA) and pWH844 (empty vector) and growth of *E.*
1111 *coli* JM109 was assessed on MSSM minimal medium with glucose and ammonium or glutamate as
1112 carbon and nitrogen source. (B) Growth assay of *B. subtilis* glutamate transporter mutants. *B. subtilis*
1113 strains were cultivated in MSSM minimal medium with 0.1 mM KCl and ammonium. Cells were
1114 harvested, washed, and the OD_{600} was adjusted to 1.0. Serial dilutions were dropped onto MSSM
1115 minimal plates with the indicated potassium concentration and ammonium or glutamate (1, 5, or 20
1116 mM). (C) Determination of glutamate transporter kinetics. The growth rates of *B. subtilis* strains
1117 expressing either AimA (upper panel) or GltT (lower panel) as the only glutamate transporter were
1118 used to determine the apparent glutamate transporter kinetics of AimA and GltT. A *B. subtilis* strain
1119 lacking all glutamate transporters (Δ*gltT* Δ*aimA* Δ*gltP*; light grey) served as a control. The strains were
1120 grown in MSSM minimal medium with 0.1 mM or 5 mM KCl and various glutamate concentrations. The
1121 growth rate was plotted against the glutamate concentration. (D) Kinetic parameters (K_S and v_{max}
1122 values) for AimA and GltT. (E) Expression of *gltT*, *aimA*, and *gltP*. The expression levels of the genes
1123 encoding the glutamate transporters GltT, AimA, and GltP were extracted from the transcriptomic
1124 analysis.
1125
1126

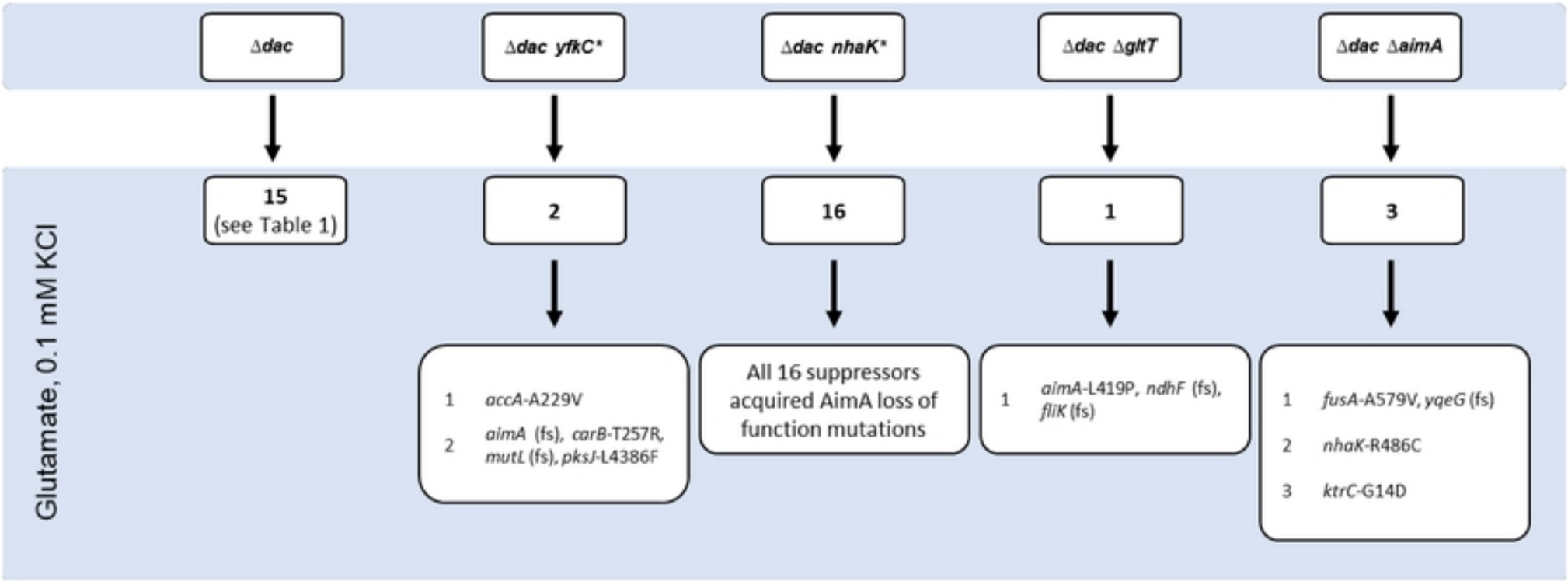

Figure 1, Krüger et al., 2020

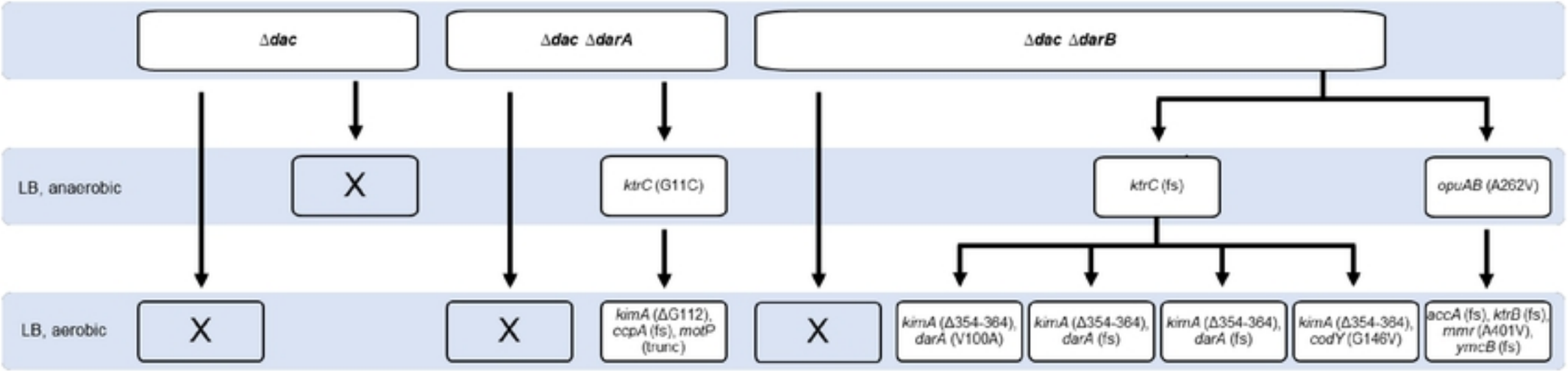

Figure 2, Krüger et al., 2020

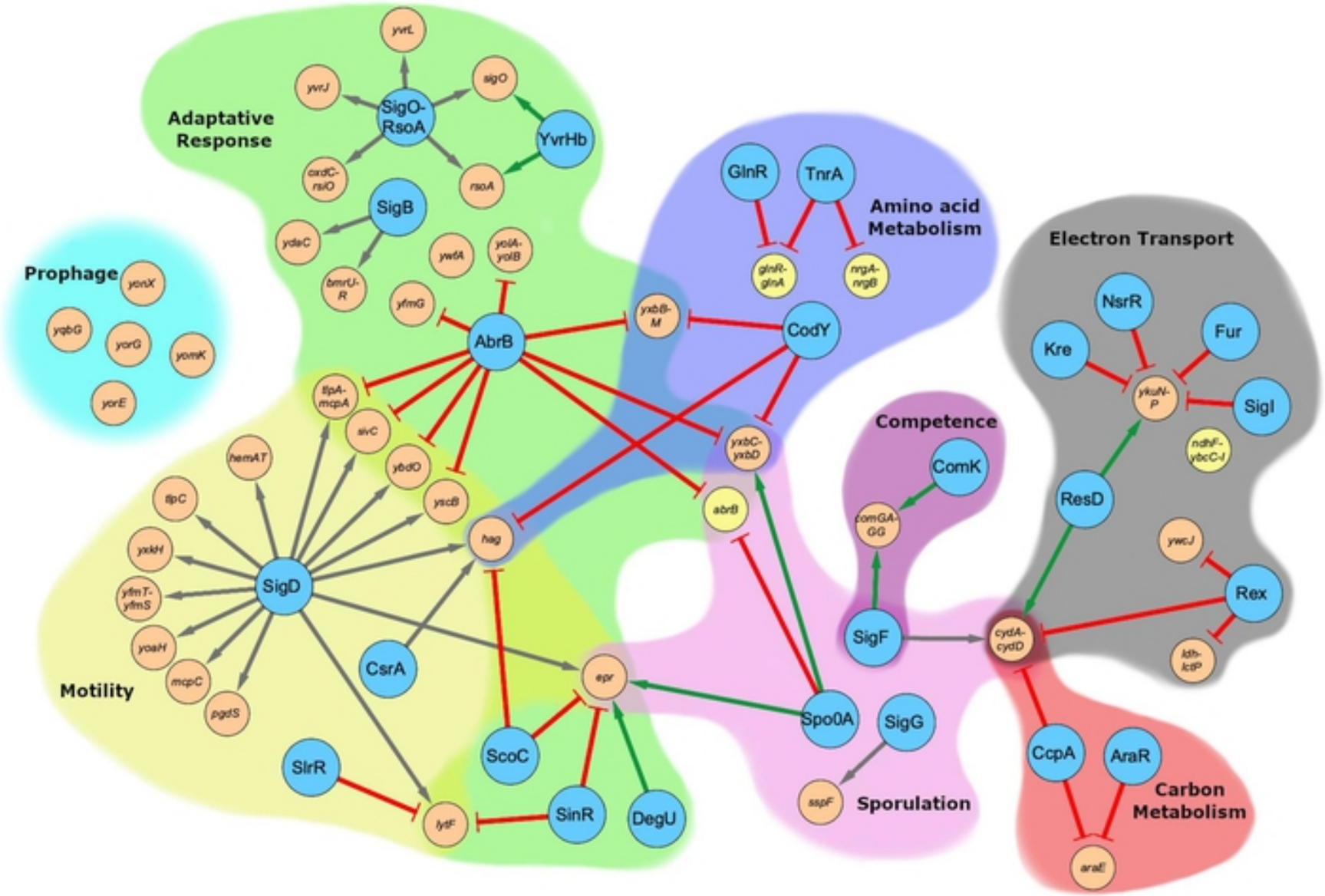

Figure 3, Krüger et al., 2020

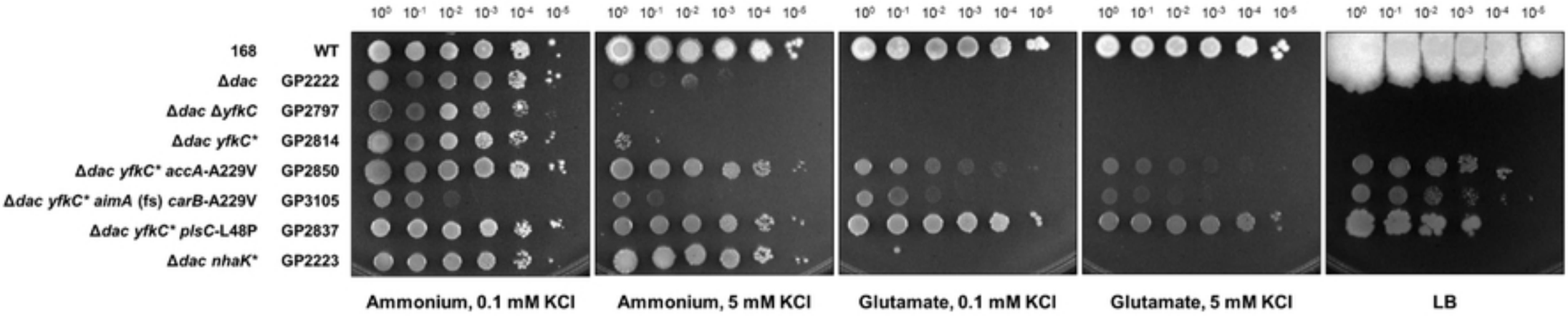

Figure 4, Krüger et al., 2020

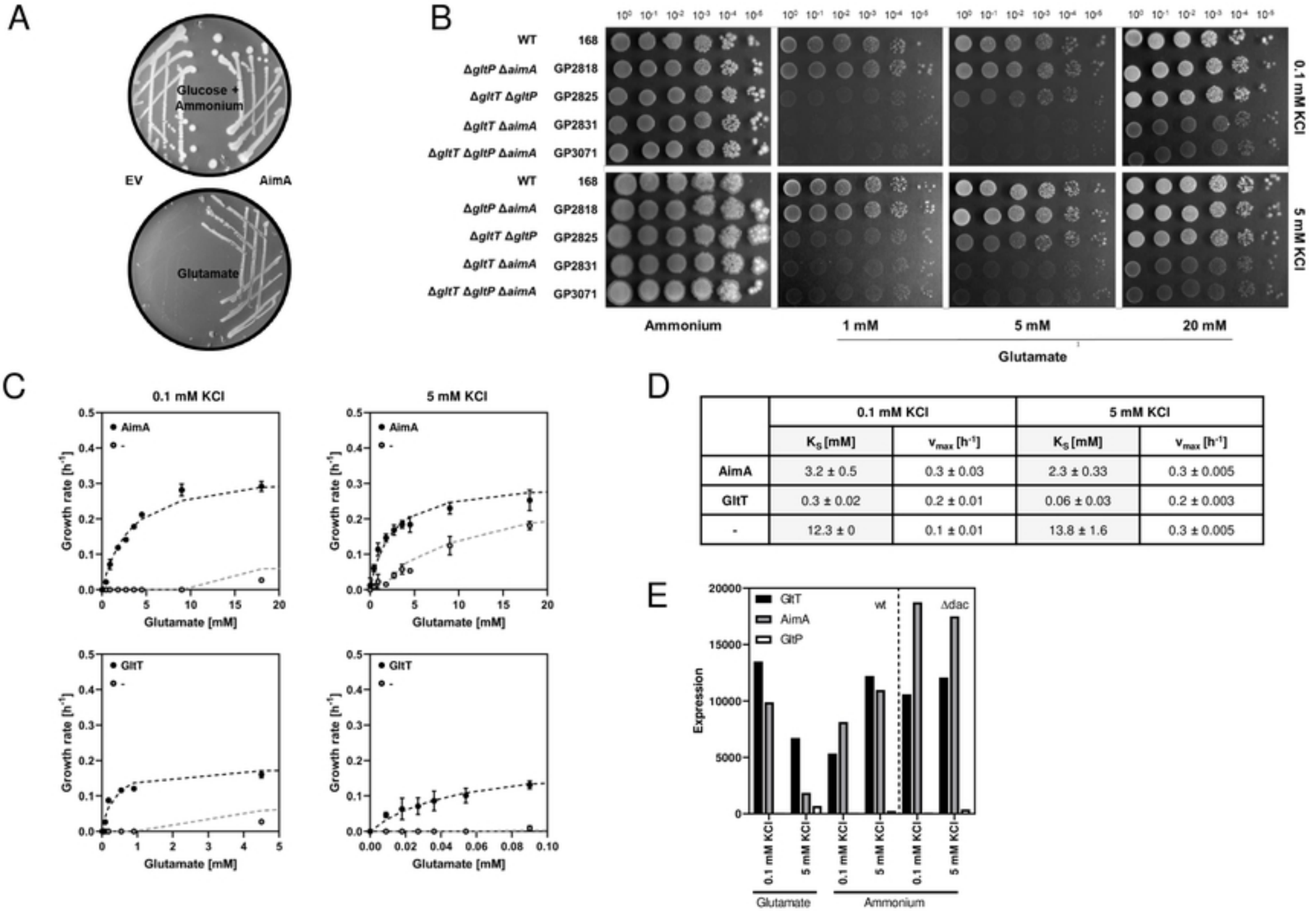

	0.1 mM KCl		5 mM KCl	
	K_S [mM]	v_{max} [h^{-1}]	K_S [mM]	v_{max} [h^{-1}]
AimA	3.2 ± 0.5	0.3 ± 0.03	2.3 ± 0.33	0.3 ± 0.005
GltT	0.3 ± 0.02	0.2 ± 0.01	0.06 ± 0.03	0.2 ± 0.003
-	12.3 ± 0	0.1 ± 0.01	13.8 ± 1.6	0.3 ± 0.005

Figure 5, Krüger et al., 2020